İSTANBUL TECHNICAL UNIVERSITY ★ INSTITUTE OF SCIENCE AND TECHNOLOGY

GAMMA-RAY DETECTOR ARRAY

M.Sc. Thesis by
Ekrem Oğuzhan ANGÜNER
(509051105)

Department : Physics Engineering
Programme: Physics Engineering

FEBRUARY 2008

İSTANBUL TECHNICAL UNIVERSITY ★ INSTITUTE OF SCIENCE AND TECHNOLOGY

GAMMA-RAY DETECTOR ARRAY

M.Sc. Thesis by
Ekrem Oğuzhan ANGÜNER
(509051105)

Date of submission : 24 December 2007

Date of defence examination : 4 February 2008

Supervisor (Chairman) : Assoc. Prof. Dr. Cenap Ş. ÖZBEN

Members of the Examining Committee : Prof.Dr. Ayşe ERZAN SİLİER

Assoc. Prof.Dr. Altuğ ŞİŞMAN

FEBRUARY 2008

İSTANBUL TEKNİK ÜNİVERSİTESİ ★ FEN BİLİMLERİ ENSTİTÜSÜ

GAMA ALGILAYICISI SERİSİ

YÜKSEK LİSANS TEZİ

Ekrem Oğuzhan ANGÜNER

(509051105)

Tezin Enstitüye Verildiği Tarih : 24 Aralık 2007

Tezin Savunulduğu Tarih : 4 Şubat 2008

Tez Danışmanı : **Doç.Dr. Cenap Ş. ÖZBEN**

Diğer Jüri Üyeleri : **Prof.Dr. Ayşe ERZAN SİLİER**

Doç.Dr. Altuğ ŞİŞMAN

ŞUBAT 2008

ACKNOWLEDGEMENT

I would like to express my deep appreciation and thanks to my advisor, Cenap Ş. Özben, for all his supports during my master thesis. I also want to thank to Mehmet Erhan Emirhan and Selçuk Hacıömeroğlu for their helps in my studies. Finally, a special thanks to my mother F.Bilge Gürdal and my aunt Ege Sunal for their endless support in all my lifetime.

December 2007 Ekrem Oğuzhan ANGÜNER

TABLE OF CONTENTS

ABBREVIATIONS

AC	: Alternative Current
ADC	: Analog to Digital Converter
Am-241	: Americium-241
Atm	: Atmosphere
Ba-133	: Barium-133
CM	: Common Mode
CMR	: Common Mode Rejection
Co-60	: Cobalt-60
Cs-137	: Cesium-137
DAQ	: Data Acquisition
DC	: Direct Current
DSP	: Digital Signal Processing
ESD	: Electro Static Discharge
eV	: Electron Volt
FWHM	: Full Width at Half Maximum
GBW	: Gain Bandwidth
G-M	: Geiger Muller
I/O	: Input / Output
LED	: Light Emitting Diode
LLD	: Lower Lever Discriminator
MCA	: Multi-Channel Analyzer
NEP	: Noise Equivalent Power
NSC	: National Semiconductor
Op-Amp	: Operational Amplifiers
PCB	: Printed Circuit Board
Pcs	: Compton Scattering Occurrence Probability
PIN	: Positive-Intrinsic-Negative
PMT	: Photo Multiplier Tube
PNP	: p-Nitro phenol
Ppe	: Photoelectric Effect Occurrence Probability
Ppp	: Pair Production Occurrence Probability
QE	: Quantum Efficiency
RFI	: Radio Frequency Interference
S/N	: Signal-to-Noise
SCA	: Single-Channel Analyzer
Selguide	: Selector Guide
Si	: Silicon
SMD	: Surface Mount Device
TI	: Texas Instruments
ULD	: Upper Level Discriminator

LIST OF TABLES

LIST OF FIGURES

LIST OF SYMBOLS

A : Gain of the op-amp
A_d : Photodiode active area
A_s : Activity of the source
A_v : Voltage gain
B : Noise bandwidth
C_0 : Feedback capacitance
C_1 : First shaping amplifier capacitance
C_2 : Second shaping amplifier capacitance
C_3 : Third shaping amplifier capacitance
C_f : Feedback capacitor
C_j : Junction capacitance
D : Detectivity of the photodiode
D* : Specific detectivity
E_0 : Energy corresponding to the center of the peak
E_{avg} : Average energy
E_g : Band-gap energy
E_{max} : Maximum energy of Compton electrons
e_n : Voltage noise
G_{os} : Offset gain
I_b : Bias current
I_{cc} : Power supply current
I_{DC} : DC current through the junction
I_f : Forward current through diode
I_{FL} : Flicker noise current
I_g : Current flowing over gain resistance
I_j : Thermal (or Johnson) noise current
I_n : Total noise current
I_o : Output current
I_p : Light generated photocurrent
I_{pulse} : Rise time associated with the RC time constant
I_s : Shot noise current
I_{sat} : Photodiode reverse saturation current
I_{sc} : Shortcut current
I_{sh} : Shunt current
k : Boltzmann's constant ($1,38.10^{-23}$ J / K)
m_e : Mass of the electron ($9,1.10^{-31}$ kg)
N : Gamma-ray flux
q : Electron charge ($1,6.10^{-19}$ C)
Q_{det} : Charge collected in the detector's capacitance
R_1 : Bias resistor
R_2 : Grounding resistor
R : Responsivity of the photodiode

R_f : Feedback resistance
R_g : Gain resistance
R_i : Finite input resistance of the op-amp
R_{Load} : Load resistance
R_s : Series resistance
R_{sh} : Photodiode shunt resistance
S_r : Peak radiant sensitivity
t_g : Gross count time
t_b : Background count time
T : Absolute temperature (K)
T_{cc} : Charge collection time
T_{diff} : Diffusion time
T_f : The time required for the output to fall from 90% to 10% of its on state value
T_p : Peaking time
T_{pulse} : Charge collection time
T_r : The time required for the output to rise from 10% to 90% of its final value
T_{rc} : Rise time associated with the RC time constant
V_{bias} : Bias voltage
V_{cc} : Power supply voltage
V_f : Forward voltage drop across diode
V_{in} : Input voltage
V_o : Output voltage
V_{oc} : Open circuit voltage
V_{os} : Offset voltage
V_s : Source voltage
W : Work function of the material
X_c : Capacitor impedance
Z_{abs} : Atomic number of the absorber
Z_f : Feedback impedance
Z_i : Input impedance
Z_o : Output impedance
ΔE : Width of the peak halfway between the baseline and the top of the peak
ε_{abs} : Absolute efficiency
ε_{int} : Intrinsic efficiency
μ : Absorption coefficient
σ : Absorption cross section
τ : RC circuit time constant

GAMMA-RAY DETECTOR ARRAY

SUMMARY

The detection of the gamma radiation with practical and low cost methods is still a point of interest for the scientists and engineers who work on this field. Especially, in the last decade, improved solid state technology have provided the new generation parts which can be used in the radiation detection devices. The purpose of this study was to design and to produce a low cost gamma-ray detector by using silicon PIN photodiodes and on-shelf components.

The basic principle of the detection is based on the interaction of the gamma-rays with the electrons in the crystal lattice. The value of induced photocurrent, caused by an incident gamma radiation, in the silicon substance with typical thickness of 100-300 μm is only a few pA. Therefore, it is generally hard to separate this induced photocurrent from the noise and to process it to obtain an observable signal. The signal-to-noise ratio of the produced detector is roughly two for 60 keV gamma energy of Am-241. Although the detection efficiency is only 2% at 60 keV, it is good enough to use it for the general-purpose monitoring type of applications and for the student experiments in the nuclear physics laboratory. Each detector has an analog output that gives energy information of the radiation and a digital output which provides count rate of the incoming radiation.

Si-PIN photodiodes used as gamma-ray detectors were designed and constructed such a way that they can run independently. Because of their low efficiency, these detectors can be connected together to make a detector array when higher detection efficiency is needed. Our detector array consists of 16 independent detectors and the data from this array is transferred to a computer with a custom designed combinational logic circuit and an 8255 interface card. This card can be installed to an ISA bus in a PC and provides data input/output for 24 bits. Thus, count rates from the individual detectors are stored in a computer. This detector array for instance can be used for monitoring the beam position in high-energy physics experiments. A single detector can be useful for monitoring of the radon activity in the fault lines or monitoring gamma activity of water circulation of a nuclear reactor.

GAMA IŞINI ALGILAYICISI SERİSİ

ÖZET

Gamma radyasyonunun pratik ve ucuz metodlar ile algılanması, bu konuda çalışan bilim adamları ve mühendisler için halen güncel bir konu olmaya devam etmektedir. Katı hal teknolojisindeki gelişmeler ışığında üretilen yeni nesil elemanlar, bu amaç için özellikle son on yıldır yaygın olarak kullanılmaktadır. Bu çalışmada, silikon PIN fotodiyotlar ve özel sipariş gerektirmeyen devre elemanları kullanılarak, düşük maliyetli ve çok amaçlı bir gama dedektör sisteminin tasarımı ve üretimi amaçlanmıştır.

Gama ışınlarının kristal örgü içindeki elektronlar ile etkileşmesi sonucu oluşan foto-akım, dedeksiyonun temel prensibidir. Gama radyasyonunun genelde fotodiyotlarda kullanılan 100-300 mikron kalınlığındaki silikon malzemede oluşturduğu akımın değeri, sadece pikoamperler mertebesinde olup, bu akımın gürültüden ayırt edilerek gözlenebilir bir sinyal haline getirilmesi çoğu zaman oldukça zordur. Üretilen dedektörün Am-241'in 60 keV lik gama çizgisi ile ölçülen sinyal gürültü oranı yaklaşık ikidir. Dedektör verimi, 60 keV ve yukarısı için sadece %2 olmakla birlikte, bu dedektörler genel amaçlı radyasyon seviye ölçümleri için ve laboratuvarda yapılan öğrenci deneyleri için rahatlıkla kullanılabilir. Her dedektör, radyasyonun enerji bilgisinin olduğu analog çıkış ve gelen radyasyonun sayım bilgisini veren dijital çıkış bulundurmaktadır.

Gama ışını algılayıcısı olarak kullanılan silikon PIN fotodiyotlar, kendi başlarına bağımsız çalışacak şekilde dizayn edilmişlerdir. Bu dedektörler, verimi düşük olduklarından dolayı, daha yüksek algılama veriminin gerekli olduğu durumlar için birleştirilerek bir dedektör serisi haline getirilebilirler. Dedektör serimiz, 16 bağımsız dedektörün birleştirilmesi ile elde edilmiştir ve bundan elde edilen data, tasarımı yapılan bir bileşik mantık devresi ve bir 8255 arayüz kartı kullanılarak bilgisayara aktarılmaktadır. PC içindeki ISA veri yoluna monte edilebilen Intel 8255 arayüz kartı, 24 bit data giriş ve çıkışı yapabilmektedir.

Örneğin bu dedektör serisi kullanılarak, yüksek enerji fiziğinde bir parçacık demetinin pozisyonu belirlenebilir. Tek bir dedektör, fay hatlarındaki sismik kaynaklı radon aktivitesindeki değişim gibi çevresel aktivitenin ölçülmesi durumunda veya bir nükleer reaktörde soğutma suyu çevrim sisteminin gama aktivitesinin monitöre edilmesi için kullanılabilir.

1. INTRODUCTION

The purpose of this work is to produce a low cost multi-purpose gamma-ray detector. In this detector, by using market available circuit components, the cost is reduced to 20$ a piece which is much cheaper than any alternative detector systems.

The detector provides the detection of gamma-rays radiation starting from 30 keV where we determined the signal to noise ratio is one. This is the lowest detection limit of our detector since no temperature stabilization takes place in our final design. There is no upper energy limit for the detection in the expense of the efficiency. However, this detector may be used for determining the radon concentration in indoor areas.

Since it is very cheap and portable, large quantities can be produced and located into the area of interest. The data can be collected and analyzed simultaneously to obtain radon map of the area in relatively short time. There are also known methods for monitoring the radon concentration in the fault lines for the early prediction of the earthquakes. These monitoring devices are quite expensive and massive. Since the power consumption of our detector is quite small, combining the detector assembly with a radio transmitter may provide remote analysis capability of the data.

The glass window in front of the photodiode can be removed. The open structure may also be very useful for the detection of the charged particles, like alphas and betas. However we only concentrated on the detection of gamma-ray. We believe detection of the charged particles using these detectors is possible.

2. PHOTODIODES

2.1 Silicon Photodiodes

Generally, photodiodes are constructed by using semiconductor materials. The most popular semiconductor materials used for this purpose are; Silicon (Si), Gallium Arsenide (GaAs), Indium Antimonide (InSb), Indium Arsenide (InAs), Lead Selenide (PbSe) [1]. They are produced in various size and shapes depending on their field of applications. Figure 2.1 shows some of the pictures of silicon photodiodes.

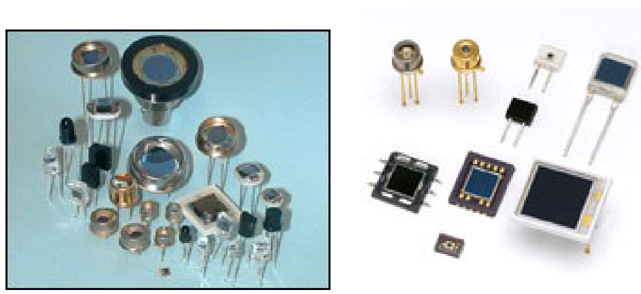

Figure 2.1 : Some Pictures of Si Photodiodes

These semiconductor materials absorb photons over a characteristic wavelength range. For example; Silicon (Si) ranges from 250 nm to 1100 nm where Gallium Arsenide (GaAs) ranges from 800 nm to 2,0 µm.

Silicon photodiodes are constructed from single crystal silicon wafers. The major difference between the ordinary photodiodes and the silicon photodiodes is silicon photodiode require silicon with less impurity. The purity of silicon is directly related to its resistivity [1].

A cross section of a typical silicon photodiode is shown in the Figure 2.2. N-type silicon is the base material. A thin p-layer is formed on the front surface of the device by thermal diffusion or ion implantation of the appropriate doping material (generally boron). Small metal contacts are applied to the front surface of the device and the entire back is coated with a metal called “anode”. The back side contact is called “cathode”. The active area of the photodiode is coated with silicon nitride, silicon monoxide or silicon dioxide to protect the active region.

It serves as an anti-reflector for incoming light. The thickness of this coating is optimized for the wavelength of the photons interested.

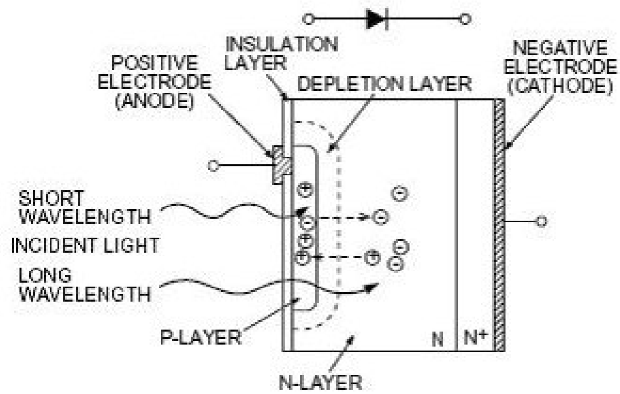

Figure 2.2 : A Cross Section of a Typical Silicon Photodiode[2]

The interface region between the p-layer and the n-layer is known as the "pn junction" (Figure 2.3).

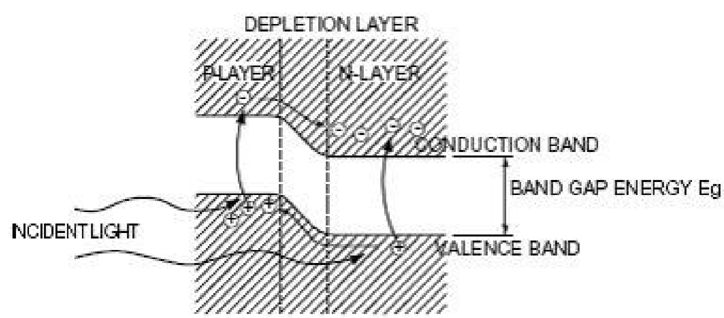

Figure 2.3 : P-N Junction of a Photodiode[2]

A PIN photodiode is a kind of photodiode which has an intrinsic (or undoped) region in between the n and p-doped regions.

2.2 Operation Principles of Silicon Photodiodes

The p-layer material and the n-layer material together form a p-n junction where the effective photoelectric conversion (forming an electron hole pair as a result of the interaction of the incident photon) takes place. The general p-layer section for silicon photodiodes are formed by diffusion of boron, thickness of approximately 1 μm or less. The undoped (or neutral) region between the p and n-layers is known as the "depletion layer".

The spectral response of the photodiode can be controlled by changing the thickness of the outer p-layer, n-layer and bottom N_+, N_- layer as well as the doping concentration.

When photons enter the photodiode through the thin p-type layer, the electrons in the crystal structure are stimulated by the incoming photons. If the photon energy is greater than the band gap energy E_g, the electrons are excited to the conduction band, leaving holes in their location in the valence band. These electron-hole pairs are called as “the carriers” and they are immediately separated and swept across the junction by the natural internal electric field formed by the charge concentration gradient. The absorption causes incoming photon intensity to drop exponentially with the penetration depth. These electron-hole pairs occur throughout the p-layer, depletion layer and n-layer materials.

Charge carriers created outside the depletion region will move randomly, many of them eventually entering the depletion region to be swept rapidly across the junction. Some of them will recombine and disappear without reaching the depletion region. In the depletion layer, internal electric field accelerates these electrons to the n-layer and the holes to the p-layer. The electrons drifted from the electron-hole pairs generated in the n-layer, and the electrons from the p-layer, are left in the conduction band of the n-layer. At this time, the holes are diffused from the n-layer to the depletion layer while being accelerated by the electric field. Then they are collected in the valance band of p-layer. In this manner, electron-hole pairs which are generated proportional to the amount of incoming photons are collected in the n and p-layers. This results the collection of positive charges in the p-layer and negative charges in the n-layer. If an external circuit is connected between the p and n-layers, electrons will move away from the n-layer, and holes will move away from the p-layer. These electrons and the holes generate a current flow in the circuit [2].

2.3 Equivalent Circuit for a PIN Photodiode

The equivalent circuit for a PIN photodiode is shown in a Figure 2.4. Fundamentally, a photodiode is a current source when working.

The current generated by a photodiode is distributed between the internal shunt resistance (R_{sh}), internal series resistance (R_s) and the external load resistance (R_{load}).

When a reverse bias voltage (V_0) is applied, the internal effect of the diode bias vanishes. As a result, ideal current source approximation can be made.

$R_s = 0$, $R_{sh} = \propto$ and $I_0 = I_p - I_f$ **(2.1)**

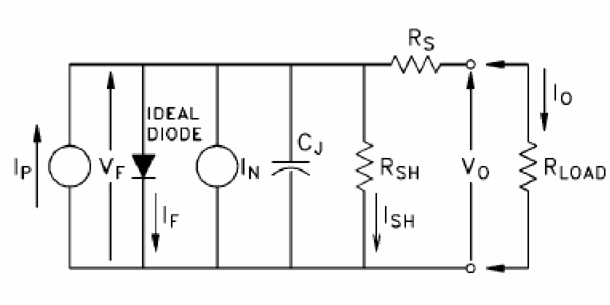

Figure 2.4 : Equivalent Circuit of a PIN Photodiode

If the external terminals are shorted together (R_{load}=0), then the short circuit photocurrent, I_{sc}, will flow [3]. In this case V_f will be equal to zero. Therefore, in the ideal case $I_{sc} = I_p$, where I_{sc} = Shortcut current, I_{sat} = Saturation Current

However in reality ;

$I_0 = I_p - I_f - I_{sh}$ **(2.2)**

$$I_{sc} = I_p - I_{sat}\left[\exp\left(q\frac{V_f}{kT}\right) - 1\right] - I_{sc}\frac{R_s}{R_{sh}} \quad \textbf{(2.3)}$$

Since V_0 = 0, V_f will be equal to $V_f = I_{sc} R_s$. Hence;

$$I_{sc} = I_p - I_{sat}\left[\exp\left(q\,I_{sc}\frac{R_s}{kT}\right) - 1\right] - I_{sc}\frac{R_s}{R_{sh}} \quad \textbf{(2.4)}$$

Note that in equation 2.4, 2^{nd} and 3^{rd} terms spoil the linearity of I_{sc}. These terms become negligible for most values, since R_s and $1/R_{sh}$ are too small.

The open circuit voltage V_{oc} is defined by the output voltage when I_0 = 0. It can be calculated by the formula

$$V_{oc} = \left(\frac{kT}{e}\right)\mathrm{Ln}\left[\frac{I_p - I_{sh}}{I_{sat}} + 1\right] \quad \textbf{(2.5)}$$

If I_{sh} is negligible, since I_{sat} increases exponentially with respect to the temperature, V_{oc} is inversely proportional to the temperature and proportional to the log of I_p.

2.3.1 Shunt Resistance

Shunt resistance means a low-resistance connection between two points in an electric circuit that forms an alternative path for a portion of the current. The shunt resistance, or dynamic junction resistance at zero voltage, can be determined by applying a small voltage to the photodiode and measuring the resulting current. This value is generally 10 mV. The values of shunt resistance can range from 100 kΩ to 100 GΩ.

The noise levels and the linearity of the short circuit photocurrent are directly related to the value of the shunt resistance as can be seen from equation 2.4. The shunt resistance is voltage dependent and used for calculating the offset gain in transimpedance amplifier circuits [3]. This offset gain can be calculated as;

$$G_{os} = 1 + \frac{R_f}{R_{sh}} \tag{2.6}$$

The value of the shunt resistance depends on the active area of the diode chip. It is also temperature dependent and measurements show that it decreases with increasing temperature.

2.3.2 Junction Capacitance

The junction capacitance of a photodiode is analogous to a parallel plate capacitor in which the spacing between the plates is a function of applied voltage. Therefore a “capacitance” is associated with the depletion region which exists at the P-N junction. The capacitance is therefore proportional to junction area and inversely proportional to the depletion region width. When the reverse bias voltage is applied to the photodiode, the depletion region will expand and the junction capacitance will decrease. The capacitance will continue to decrease with increasing reverse bias voltage applied, until the depletion region expands all the way to the back surface of the photodiode. At this point the capacitance of the photodiode becomes nearly constant [3].

2.3.3 Response Time of a Photodiode

The response time of a photodiode is defined as the time required for light generated carriers to cross the P-N junction.

In many applications, response time is limited by the RC time constant calculated from the multiplication of the detector capacitance and series resistance plus load resistance in the operating circuit.

It is a common way to express the response time in terms of the rise time or the fall time where the rise time of a photodiode consists of three components:

1. T_{CC} is the time required for the internal electric field to sweep out carriers generated within or entering the depletion region. Typically T_{CC} is less than 1 ns [3].

2. T_{RC} (rise time associated with the RC time constant) is the time required to charge or discharge the junction capacitance (C_j) of the photodiode through the external load resistance (R_{load}) and is given as in [3] ;

$$T_{RC} = 2.2\, R_{Load}\, C_j \tag{2.7}$$

R_{load} term consists of the series combination of the external load resistance and the internal series resistance of the photodiode (R_s). The C_j term should include not only the junction capacitance of the photodiode but also all external capacitances such as the packaging capacitance and the external wiring capacitance.

3. T_{dif} (diffusion time) is the time needed for carriers generated outside the depletion region to diffuse into the depletion region [3].

The total risetime of a photodiode is equal to the square root of the sum of the squares of the three risetime components as in equation 2.8.

$$T_r = \sqrt{\left[T_{cc}^2 + T_{rc}^2 + T_{dif}^2\right]} \tag{2.8}$$

2.4 Noise Characteristics of a Photodiode

Here are some noise characteristic concepts and noise types that can be seen in the photodiode circuits.

2.4.1 Dark Current

Dark current is the current through the photodiode in the absence of any optical signal, when it is operated in photoconductive mode. The dark current includes photocurrent generated by background radiation and the saturation current, I_{sat}.

It is also a source of noise when a photodiode is used in optical communication or detection systems. To overcome the dark current problem, generally a reverse bias voltage is applied across the junction. This voltage may be as low as 10 mV or as high as 50 V and the dark currents may vary from pA to μA depending on the photodiode active area. The dark current is temperature dependent. The rule of thumb is that the dark current will approximately double for every 10 °C increase in temperature.

2.4.2 Noise Current

The main noise sources in photodiodes are; thermal noise (or Johnson noise), shot noise and flicker noise (1/f or contact noise).

These noise sources are independent of each other and the total noise current is the root of the sum of the square of each of these noise sources as shown in equation 2.9.

$$I_n = \sqrt{I_j^2 + I_s^2 + I_f^2} \tag{2.9}$$

2.4.3 Thermal (or Johnson) Noise Current

Thermal noise is a fundamental physical phenomenon caused by the random thermal motion of electrons and can occur in any linear passive resistor [3]. Photodiode thermal noise is caused by its shunt resistance R_{sh} and is directly proportional to absolute temperature as in equation 2.10.

$$I_j = \left[4 \frac{kTB}{R_{sh}} \right] \tag{2.10}$$

Where B = Noise Bandwidth and R_{sh} = Value of the shunt resistance

In photodiodes, Johnson noise may become the dominant type when either low leakage/high dynamic resistance photodiodes are used in the zero bias configurations or when high value resistors (MΩ to GΩ) are used as current sensing elements [3,4]. Because thermal noise is independent of frequency and contains constant noise power density per unit bandwidth, it is considered as white noise and is expressed in units of amps per square root Hertz.

For example, a photodiode having R_{sh} = 0, 5 MΩ at 25 °C:

$$\frac{I_j}{\sqrt{B}} = \sqrt{\frac{4kT}{R_{sh}}} \quad \textbf{(2.10a)}$$

$$\frac{Ij}{\sqrt{B}} = 0{,}18\ \frac{pA}{\sqrt{Hz}} \quad \textbf{(2.10b)}$$

2.4.4 Shot Noise Current

Shot noise is caused by the random fluctuations in the normal current flow through the P-N junction. A noise current is generated because of each electron carries a discrete amount of charge and the flow of electrons are subject to small random fluctuations. It has been shown that shot noise can be expressed by the equation 2.11.

$$I_s = \sqrt{2qI_{DC}B} \quad \textbf{(2.11)}$$

Shot noise is independent of frequency and is also called as white noise like thermal noise. Shot noise may become important when either high leakage photodiodes are used in reverse bias or when measurements include very weak signal detection.

2.4.5 Flicker (or l/f) Noise Current

Flicker noise is the least understood noise type. It is usually attributed to manufacturing noise mechanisms or surface effects of the device [3]. Experimental data show that this type of noise has a dependence on DC current and is similar to shot noise. A general equation for this type of noise is given in equation 2.12.

$$I_{fl} = \sqrt{\frac{K\,I_{DC}\,B}{f}} \quad \textbf{(2.12)}$$

In equation 2.12, K is defined as a constant that depends on the type of material and its geometry.

Different than thermal and shot noises, flicker noise has 1/f spectral density. In the ideal case for which it is exactly proportional to 1/f, it is called "pink noise".

The constant (K) can only be determined empirically and may differ greatly even for similar devices. Flicker noise may dominate when the bandwidth of interest contains frequencies less than about 1 kHz.

2.4.6 Noise Equivalent Power of a Photodiode

The lowest limit of the light detection for a photodiode is defined as the incident light intensity required to generate a current equal to the noise current. This limit is called "Noise Equivalent Power", NEP and it is formulated as in equation 2.13.

$$NEP = \frac{I_n}{S_r} \tag{2.13}$$

NEP values range from about 10^{-15} for small area, low noise silicon photodiodes, to over 10^{-12} for large area cells.

2.4.7 Detectivity of a Photodiode

Detectivity or in the other words "detection capability" (D) of a photodiode is given by the inverse value of NEP. The detectivity is defined as the minimum detectable radiant power or minimum detector signal to noise ratio [3]. A photodiode with a high D value indicates that the ability of low level detection. Detectivity is formulated as in equation 2.14.

$$D = \frac{1}{NEP}\left(\frac{\sqrt{Hz}}{W}\right) \tag{2.14}$$

Noise is proportional to the square root of the photosensitive area. This means the smaller the photosensitive area (A_d) is, the better the NEP and the detectivity is. The specific detectivity which is shown as $D^{\otimes}$ (D-Star) defines an area independent new concept.

By definition;

$$D^{\otimes} = D\sqrt{A_d} \tag{2.15}$$

2.5 Photodiode Responsivity and Spectral Response

The measure of sensitivity, is the ratio of radiant energy (in watts) incident on the photodiode to the output photocurrent (in amperes). It is expressed as the absolute responsivity in amperes per watt. Note that radiant energy is expressed as $(\frac{W}{cm^2})$ and the photodiode current as $(\frac{A}{cm^2})$. The cm^2 term cancels and we get (A/W). A typical responsivity curve of a photodiode which shows A/W as a function of the wavelength is given in Figure 2.5 [5]. It shows that the responsivity depends on the applied bias voltage.

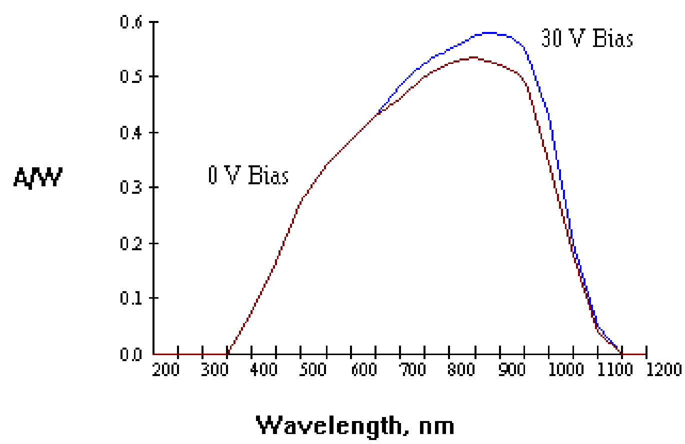

Figure 2.5 : Responsivity Curve of a Photodiode[6]

As explained in the operation principles of Si photodiodes, when the energy of absorbed photons is lower than the band gap energy E_g, the photovoltaic effect does not occur. The limiting wavelength λ_h can be expressed in terms of E_g by equation 2.16.

$$\lambda_h = \frac{1240}{E_g} \text{ (nm)} \qquad \textbf{(2.16)}$$

The wavelength of the radiation to be detected is an important parameter. Energy gap for silicon is 1,12 eV at the room temperature. Hence the limiting wavelength will be 1100 nm. As can be seen from the Figure 2.5, silicon becomes transparent to radiation of longer than 1100 nm wavelength. The amount of photon absorption within the surface layer becomes very large for the shorter wavelengths. Therefore for getting the higher sensivity, thinner surface layers are used.

Also the P-N junctions are constructed close to the surface. For ordinary photodiodes the cut-off wavelength is 320 nm [5].

The cut-off wavelength is determined by the intrinsic material properties that are used in the photodiode, but it is also affected by the spectral transmittance of the window material. For borosilicate glass and plastic resin coating, wavelengths below 300 nm are absorbed. If these materials are used as the window, the short wavelength sensitivity will be lost. For wavelengths below 300 nm, photodiodes with quartz windows are used. For visible light region measurements, a visual-compensation filter is used as the window.

2.6 Quantum Efficiency of a Photodiode

Quantum Efficiency (QE) is a quantity defined for photosensitive devices as the percentage of photons hitting the photoreactive surface that produce electron–hole pairs. It is an accurate measurement of the sensitivity of the device and often measured over a range of different wavelengths to characterize the energy behavior of the system. The sensitivity of a photodiode is expressed in the units of amperes of photodiode current per watt as told in previous section. The QE is related to the responsivity of the photodiode by the following equation

$$QE\,(\%) = 1{,}24 \cdot 10^{5} \cdot \frac{R}{\lambda} \qquad \textbf{(2.17)}$$

Note that both the quantum efficiency and the responsivity are the functions of the wavelength of the incoming photons. Operating under ideal conditions of reflectance, crystal structure and internal resistance, a high quality silicon photodiode of optimum design would be capable of approaching a QE of 80% [5].

2.7 Reverse Bias Connection in Si Photodiode

Connecting the P-type region to the negative terminal of the battery and the N-type region to the positive terminal produces the reverse-bias effect. The connections are illustrated in the Figure 2.6.

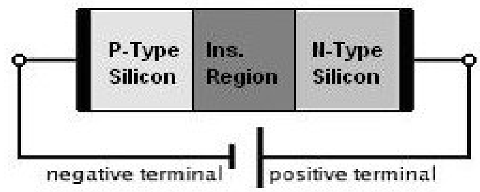

Figure 2.6 : Reverse Bias Connection

Because the negative terminal of the power supply is connected to P-type region, the holes in the P-type region are pulled away from the junction. Hence, the width of the non-conducting depletion region increases. Similarly, because the N-type region is connected to the positive terminal, the electrons will also be pulled away from the junction. This effect increases the potential barrier and the electrical resistance against the flow of charge carriers. For this reason, there will be minimal electric current across the junction.

As the reverse bias voltage increases, the depletion region expands. The electric field grows as the reverse voltage increases. When the electric field increases beyond a critical level, the junction breaks down and current begins to flow. Breakdown voltage is defined as the voltage at which the dark current becomes nearly 10 µA for small active area photodiodes. These breakdown processes are non-destructive and reversible as long as the current density does not exceed levels that can cause thermal damage.

A photodiode signal can be measured as voltage or current. Current measurement gives better linearity, offset and bandwidth performance. The photocurrent generated needs to be converted to voltage using a transimpedance configuration.

The photodiode can be operated with or without an applied reverse bias depending on the specific requirements of the application. They are named by "Photoconductive Mode" (bias applied) and "Photovoltaic Mode" (no bias applied).

2.7.1 Photoconductive Mode

If a high speed of response is required for a measurement with a photodiode, it is better to operate it with reverse bias in the photoconductive mode. This is due to the increase in the depletion region width.

Consequently decrease in junction capacitance with increasing bias. The generated photocurrent produces a voltage across a load resistor. The main disadvantage of this mode of operation is the increased leakage current due to the increasing bias voltage, giving higher noise than the photovoltaic mode [7]. Typical photoconductive mode connection of the photodiode is given in Figure 2.7.

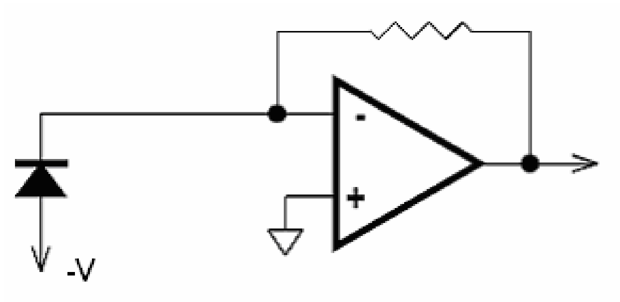

Figure 2.7 : Photoconductive Mode Connection Schematic

2.7.2 Photovoltaic Mode

The photovoltaic mode of operation, where the reverse bias is not used, is used when the measurement is based on low frequency applications (<350 kHz) as well as ultra low light level applications [7]. The photocurrents in this mode of operation have less variation in responsivity with temperature. Because there is no leakage current, photovoltaic mode is used when the noise is more important to take into account. The connection schematic of the photovoltaic mode is given in Figure 2.8.

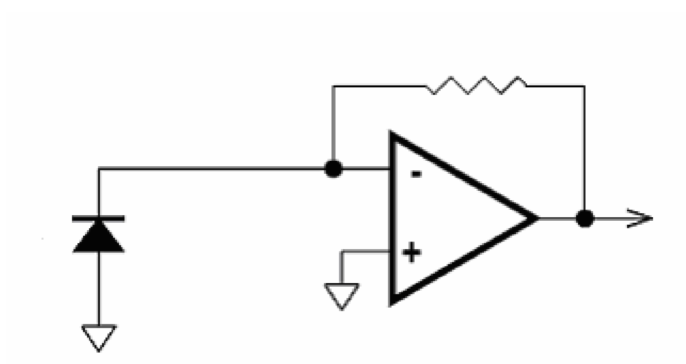

Figure 2.8 : Photovoltaic Mode Connection Schematic

2.8 Temperature Characteristics of a Photodiode

Temperature changes greatly affect the sensitivity of the photodiode and the dark current. The changes in the sensivity and the dark current are related to the temperature dependent light absorption coefficient.

For long wavelengths, sensitivity increases with increasing temperature. This increase becomes prominent at wavelengths longer than the peak wavelength. For short wavelengths, sensivity decreases.

Because valence band electrons are excited with respect to temperature changes, they are pulled into conduction band with increasing temperature. Dark current gradually increases with temperature as shown in the Figure 2.9. This indicates a twofold increase in dark current for a temperature rise from 5 °C to 10 °C. This also means a reduction of the shunt resistance R_{sh} and a rise in the thermal and the shot noise [2].

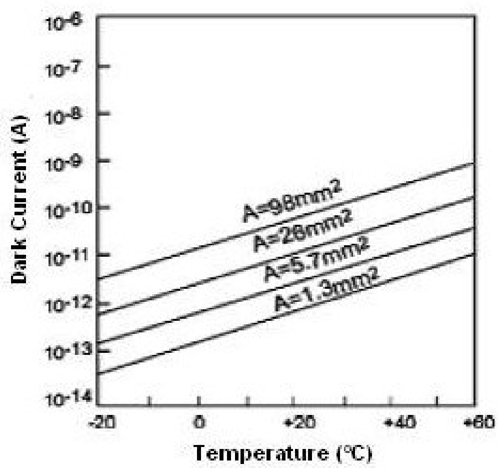

Figure 2.9 : Dark Current versus Temperature characteristics of a Photodiode[2].

Because of the rise in the dark current and the reduction in the shunt resistance with increasing temperature, it is necessary to consider the system design for the maximum operating temperature. It is generally stated that the dark current doubles for every 10 °C increase in temperature. However, since the dark current is made up of several components having different contributions, the net results may change between doubling it every 7 °C and 15 °C depends on the device design.

3. OPERATIONAL AMPLIFIERS

The operational amplifier, which is generally called “op-amp” is the device that produces an output voltage from the difference between the signals at two input terminals, multiplied by the gain of the op-amp. A classical op-amp schematic is given in Figure 3.1.

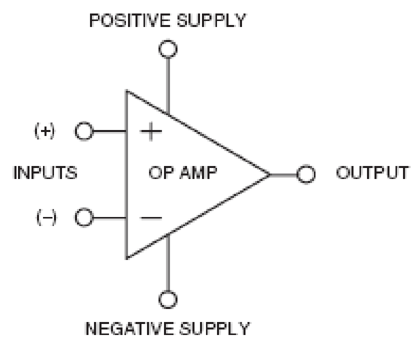

Figure 3.1 : Op-amp Schematic

The op-amp is basically a differential amplifier having a large voltage gain, very high input impedance and very low output impedance. The op-amp has an "inverting" or (-) input and "non-inverting" or (+) input and a single output. The op-amp is usually powered by a dual polarity power supply in the range of ±5 volts to ±15 volts. The gain of the op-amp (A) can vary from $10 - 10^6$.

3.1 Ideal Op-amp Assumptions

An ideal op-amp has following assumptions;

A – Infinite Gain

An ideal op amp has an infinite gain for differential input signals. Actually in real case, op-amps have quite high gain that is also called open-loop gain. This assumes that the output voltage of an op-amp can achieve any value. In reality, when the output voltage gets close to the power supply voltage, saturation occurs.

Gain is measured in terms of (V_{out}/V_{in}), and is given in the dimensionless numeric gain (V/V).

Gain is generally expressed in terms of decibel (dB), which is mathematically defined as (dB=20 log[numerical gain]). For example, a numerical gain of 10^6 is equivalent to a 120 dB gain.

100 dB – 130 dB gains are common for the most op-amps, but high-speed op-amps may have gains of 60–70 dB range. Also, an ideal op-amp has zero gain for signals common to both inputs which is called the "common-mode" (CM) signals or, stated in terms of the rejection for these common-mode signals, an ideal op-amps have infinite CM rejection (CMR). Op-amps can have CMR up to 130 dB for most devices, or this value can be as low as 60–70 dB for some high-speed op-amps.

B – Infinite Input Impedance

The ideal op-amp also has infinite input impedance. This means the bias currents (I_b) at both inputs are zero or in other words, no current ever flows into either input of the op-amp. In the reality, actual bias currents can be as low as a few fA, or as high as several µA. Some of the high-grade op-amps can have input impedance in the TΩ range.

C – Zero Output Impedance

The output impedance for an ideal op-amp should be zero or in the other words the ideal op-amp has a zero offset voltage. So the ideal op-amp acts as a perfect internal voltage source with no internal resistance which means that the op-amp can drive any load impedance to any voltage. In reality, offset voltage of the op-amps can vary between 1 µV to 1 mV. This extremely wide range of specifications reflects the different input structures used within various devices.

D – Frequency Independence

The frequency response of the ideal op amp should be flat means the gain of the op-amp does not change with frequency.

E – Infinite Bandwidth

The ideal op-amp should amplify all signals from DC to the highest AC frequencies. However bandwidth of the op-amps is rather limited. This limitation is specified by the Gain-Bandwidth product (GB), which is equal to the frequency, where the amplifier gain becomes unity. An ideal op-amp can be seen in Figure 3.2.

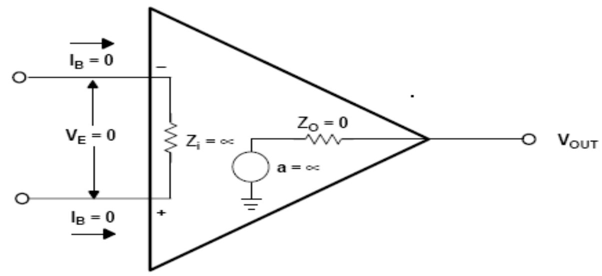

Figure 3.2 : Ideal Op-amp

3.2 Op-amp Feedback Hookups

A circuit that returns a fraction of the output signal of an electronic circuit, or control system to the input of the circuit or system is called “feedback circuit”. It is called as “positive” or “regenerative” feedback when the output signal is returned at the same phase as the input signal. When the feedback signal is in the opposite phase to the input signal, the feedback is called “negative or degenerative”.

The negative feedback used in electronic circuits produces some changes in the characteristics of the system that can improve the performance of the system. Feedback is used either to change the frequency response of an amplifier circuit for producing more uniform amplification over a range of frequencies, or to produce conditions for oscillation in electronic circuits. It is also used for stabilizing the gain of the system against the temperature and for compensating the tolerances of the circuit components.

Hence, by using the feedback circuits [8];

- The gain of the circuit can be made less sensitive to the values of the individual components.

- The effects of noise can be reduced.

- The input and output impedances of the amplifier can be modified.

- The bandwidth of the amplifier can be extended.

The feedback network that is shown in Figure 3.3 can be resistive or reactive, linear or nonlinear, or any combination of these.

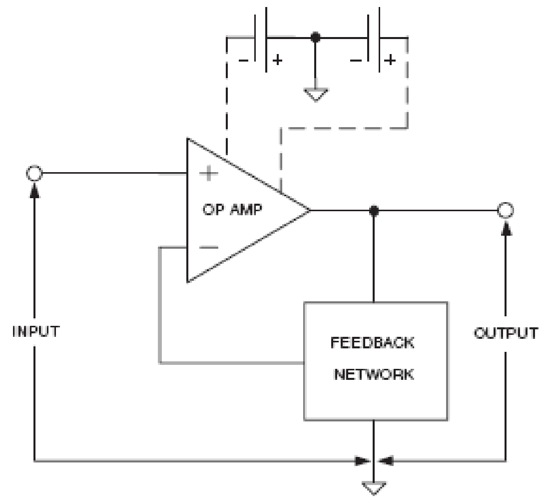

Figure 3.3 : The Feedback Network

In the op-amp use, the feedback concept is essential. The use of feedback in op-amp makes the closed-loop gain characteristics to be dependent on the external components, which reduces the dependency to the unstable amplifier open-loop characteristics.

Note that in the Figure 3.3; the input signal is applied between the op-amp (+) input and a "common" or "reference" point. It is denoted by the ground symbol. This reference point is also common to the output and feedback network [8]. By definition, the output signal of the op-amp output stage appears between the output terminal where it is feedback network input at the same time and this common ground point.

3.3 Standard Op-amp Stages

Op-amp feedback connection types can be categorized into a few basic types of connection, which include the two most used types called "non-inverting" and "inverting" stages. Using the concepts of infinite gain, zero input offset voltage, zero bias current, etc…, the standard op-amp feedback stages can be designed.

3.3.1 The Non-inverting Op-amp Stage

The non-inverting stage for op-amp which is also known as a "voltage follower with gain" or "simply voltage follower" is shown in Figure 3.4.

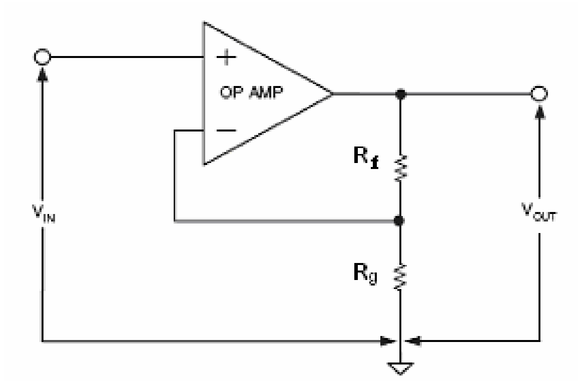

Figure 3.4 : Non-inverting Op-amp Stage Connection

The non-inverting op-amp has the input signal connected to its non-inverting input. Because of this connection, its input source sees infinite impedance. Because the negative input must be at the same voltage as the positive input, there is no input offset voltage because $V_{os} = (V_{in+} - V_{in-}) = 0$. The op-amp output drives current into R_f until the negative input is at the voltage, V_{in}. This action causes V_{in} to be appeared across R_g.

The voltage divider rule is used to calculate V_{in}. V_{out} is considered as the input to the voltage divider and V_{in} is the output of the voltage divider. Because no current can flow into an op-amp, the use of the voltage divider rule is allowed. Equation 3.1 is written from the voltage divider rule.

$$V_{in} = V_{out} \frac{R_g}{R_g + R_f} \tag{3.1}$$

From the equation 3.1, one can obtain the gain for the non-inverting op-amp where

$$A = \frac{V_{out}}{V_{in}} = \frac{R_g + R_f}{R_g} = \left(\frac{R_f}{R_g}\right) + 1 \tag{3.2}$$

If R_g is too large with respect to R_f, R_f / R_g ratio goes to zero. So the equation 3.2 can be reduced to V_{out}=1. V_{out}=1 means that the circuit has a unity gain buffer. This non-inverting gain configuration is one of the most useful of all op amp stages. V_{in} sees the op-amp's high impedance (+) input. This provides an ideal interface to the driving source. Gain can easily be adjusted over a wide range by adjusting R_f and R_g. If R_f is taken as zero and R_g open, the stage gain again becomes unity, and V_{out} is then exactly equal to V_{in}.

This special non-inverting gain case is also called a "unity gain follower" which is a stage generally used for buffering a source. Some types of op-amps are self-destructive when R_f is left out of the circuit, so R_f is used in many buffer designs. When R_f is used in a buffer circuit, its function is to protect the inverting input from an over-voltage to limit the current through the input ESD (electro-static discharge) structure (typically < 1 mA). It can have almost any value (20 kΩ is used frequently) [9]. Therefore R_f can never be left out of the circuit in a current feedback amplifier design because R_f determines stability in current feedback amplifiers.

Note that the gain is independent of the op-amp parameters. As it can be seen at equation 3.2, the gain is the function of the feedback and gain resistances. The gain can be changed by adjusting the R_f / R_g ratio. The resistor values are determined by the impedance value that in needed for the circuit.

It should be noted that this op-amp example contains only a simple resistive case of feedback. As mentioned before, the feedback can also be reactive, for example Z_f includes capacitors and/or inductors. But in all cases, it must include a DC path, if we assume the op amp is biased by the feedback.

3.3.2 The Inverting Op-amp Stage

In the inverting op-amp stage which is also known as the inverter is shown in Figure 3.5. As can be seen from the comparison of the Figures 3.4 and 3.5, the inverter can be considered as similar to a follower with a transposition of the input voltage V_{in}.

The non-inverting input of the inverting op-amp circuit is grounded. One assumption is made which is the input error voltage is zero, so the feedback keeps inverting the input of the op-amp at a virtual ground (not actual ground but acting like a ground). The current flow in the input pins is assumed to be zero, so the current flowing through R_g (I_g) equals the current flowing through R_f (I_f).

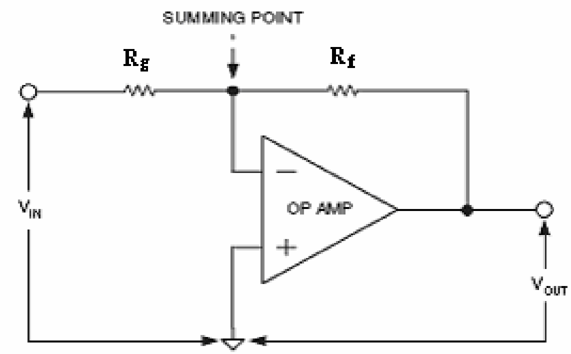

Figure 3.5 : Inverting Op-amp Stage Connection

Using Kirchhoff's law, we can write equation 3.3. The minus sign is inserted because of the inverting input.

$$I_g = \frac{V_{in}}{R_g} = -I_f = -\frac{V_{out}}{R_f} \quad \textbf{(3.3)}$$

$$G = \frac{V_{out}}{V_{in}} = -\frac{R_f}{R_g} \quad \textbf{(3.4)}$$

Note that the gain is a function of the feedback and gain resistances, so the feedback circuit has done its function of making the gain independent of the internal op-amp parameters. The resistance values are determined from the impedance level that is needed for the applied feedback circuit.

Also note that the output signal is the input signal amplified and inverted. The circuit input impedance is set by R_g because the inverting input is held at a virtual ground.

The major difference between the inverting stage and the non-inverting stage is the input to output sign reversal, which is denoted by the minus sign in equation 3.4. The inverting configuration is also one of the more useful op-amp stages. Unlike a non-inverting stage, the inverter gives relatively low impedance input for V_{in} which is the value of R_g. This factor provides a finite load to the source. While the stage gain can be adjusted by changing the values of R_f and R_g, there is a practical limitation imposed at high gain, when R_g becomes relatively low. If R_f is zero, the gain becomes zero.

The inverter's gain behavior, due to the principles of infinite op-amp gain which are zero input offset, and zero bias current etc…, gives rise to an effective node of zero voltage at the (−) input.

The input and feedback currents sum at this point, which logically results in the term summing point. It is also called a virtual ground, because of the fact it will be at the same potential as the grounded reference input [10].

Note that all op-amp feedback circuits have a summing point. The summing point is always the feedback junction at the (–) input node, as shown in Figure 3.5. However in follower type circuits, this point is not a virtual ground since it follows the (+) input. A special gain case for the inverter occurs when $R_f = R_g$, which is also called a unity gain inverter. This form of inverter is commonly used for generating complementary V_{out} signals, for example, $V_{out} = -V_{in}$.

3.4 Capacitors Used in Feedback Circuits

Capacitors are the key component in a circuit design. Capacitors have an impedance of $X_c = \dfrac{1}{2\pi f C}$. Note that when the frequency is zero, the capacitive impedance (also known as reactance) is infinite which means capacitors are open circuit for DC, and is zero when the frequency is infinite.

When a capacitor is used with a resistor, they form what is called a break-point. Without going into complicated math, just accept that the break frequency occurs at $f = \dfrac{1}{2\pi R C}$ and the gain is –3 dB at the break frequency.

The low pass filter circuit shown in Figure 3.6 which has a feedback capacitor in parallel with the feedback resistor.

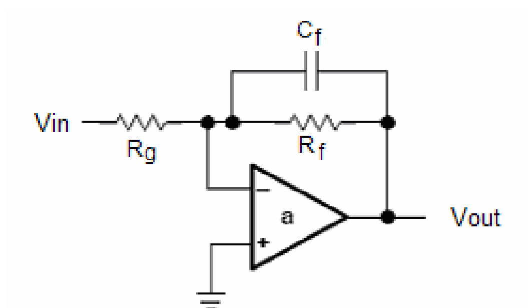

Figure 3.6 : Low-pass Filter Connection Schematic

The gain for the low pass filter is given in equation 3.5.

$$\frac{V_{out}}{V_{in}} = -\frac{X_c \parallel R_f}{R_g} \qquad \textbf{(3.5)}$$

At very low frequencies (for example DC) $X_c \rightarrow \infty$, so R_f dominates the parallel combination in equation 3.5, and the capacitor has no effect. The gain at low frequencies can be reduced to ($-R_f / R_g$). At very high frequencies $X_c \rightarrow 0$, so the feedback resistor is short circuited and gain is reduced to zero. At the frequency where $X_c = R_f$ the gain is reduced by $\sqrt{2}$ because complex impedances in parallel equal half the vector sum of both impedances [9].

Connecting the capacitor in parallel with R_g where it has the opposite effect, makes a high pass filter shown in Figure 3.7. Equation 3.6 gives the equation for the high pass filter.

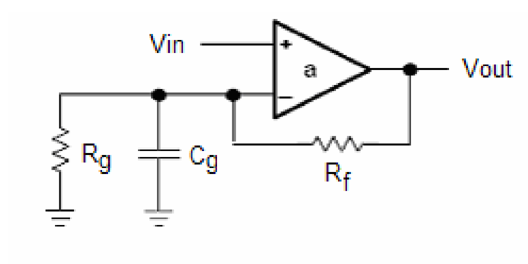

Figure 3.7 : High-pass Filter Connection Schematic

$$\frac{V_{out}}{V_{in}} = 1 + \frac{R_f}{X_c \parallel R_g} \qquad \textbf{(3.6)}$$

At very low frequencies $X_c \rightarrow \infty$, R_g dominates the parallel combination in equation 3.6, and the capacitor has no effect. The gain at low frequencies is $1 + R_f / R_g$. At very high frequencies $X_c \rightarrow 0$, and the set resistor of the gain is shorted out thus increasing the circuit gain to maximum [9].

3.5 Noise in Op-amp Circuits

The reason of using op-amp is the manipulation of the input signal in some fashion. Unfortunately in the real world, the input signal has unwanted noise imposed on it. Noise shows random characteristics, so the instantaneous value and/or phase of the waveform cannot be predicted precisely at any time.

Noise can be generated in the op-amp from its internal components or imposed on the circuit by external sources [11].

3.5.1 External Noise Sources in Op-amp Circuits

External types of noise include;

A - Conducted Emissions: Noise that is generating by the analog circuit through its connections to other circuits is called “Conducted Emissions Noise”. This is usually negligible in analog circuits, unless it is high powered (Example: an audio amplifier that takes heavy currents from its power supply).

B - Radiated Emissions: Noise that is generated or transmitted by the analog circuitry through the air is called “Radiated Emissions Noise”. This is also usually negligible in analog circuits, unless it has high frequency (Example: video amplifiers circuits).

C - Conducted Susceptibility: Noise from external circuits which is conducted into the analog circuit through its connections to other circuits is called “Conducted Susceptibility Noise”. Analog circuits must be connected to the outside world by at least a ground connection, a power connection, an input and an output. Noise can be conducted into the circuit through all of these paths.

D - Radiated Susceptibility**:** Noise that is received through the air (or transmitted into the analog circuitry) from external sources is called “Radiated Susceptibility Noise”. Analog circuits, placed on a PCB, may have high-speed digital logic including DSP chips. High-speed locks and switching digital signals create considerable radio frequency interference. Other sources of radiated noise are numberless. The switching power supply in a digital system, cellular telephones, broadcast radio and TV, fluorescent lighting, nearby PC’s, lightning in thunderstorms, and so on. Even if the analog circuit is primarily at audio frequency, RFI may produce noticeable noise in the output.

3.5.2 Noise Colors

The real op-amp noise will appear as the summation of some or all of noise types. The various noise types are difficult to separate. But there is an alternative way to describe noise, which is called color. The colors of noise come from light, and refer to the frequency content. Many colors are used to describe noise, some of them having a relationship to the real world.

White noise is in the middle of a spectrum that runs from purple to blue, to white, to pink and red/brown. These colors correspond to powers of the frequency to which their spectrum is proportional. They are shown in Figure 3.8.

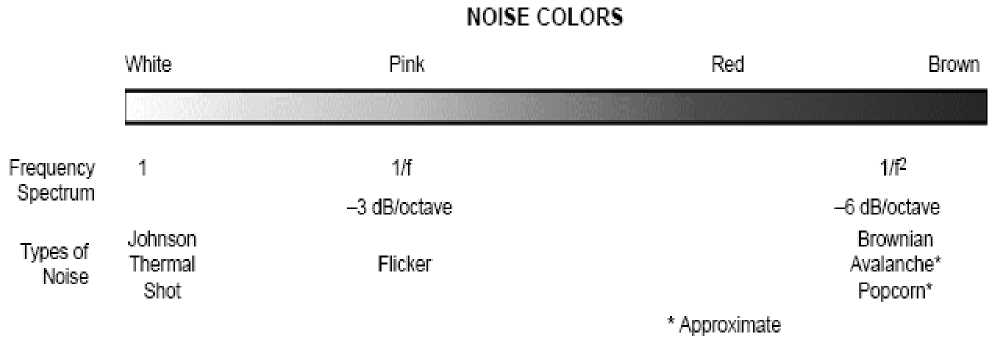

Figure 3.8 : Noise Colors[9]

A - White Noise: White noise is the noise in which the frequency and power spectrum is constant and independent of frequency. The signal power for a constant bandwidth (centered at frequency f_0), does not change if f_0 is changed. Its name comes from the similarity to white light. When it is plotted versus frequency, white noise is a horizontal line of constant value which means that it is frequency independent.

Shot and thermal (Johnson) noise sources are close to white, although there is no such thing as pure white noise. White noise has infinite energy at infinite frequencies by definition. White noise always becomes pinkish at high frequencies. Steady rainfall or radio/TV static on a channel with no broadcasting is an approximate for white noise characteristic.

B – Pink Noise: Pink noise is the noise with a (1/f) frequency and power spectrum. It has equal energy per octave (or decade for that matter). This means that the noise amplitude decreases logarithmically with frequency. Pink noise can be shown in nature. Many random events show a 1/f characteristic. Flicker noise displays 1/f characteristic too.

3.5.3 Signal to Noise Ratio

Consider a chain of two amplifiers with gains A_1 and A_2, and input noise levels N_1 and N_2. A signal S is applied to the first amplifier, so the input signal to noise ratio is (S/N_1).

The chain of two amplifiers is shown in Figure 3.9

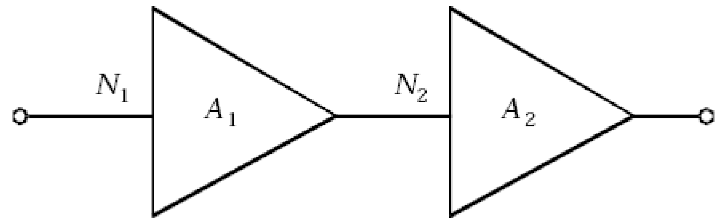

Figure 3.9 : The Chain of Two Amplifiers

$$\left(\frac{S}{N}\right)^2 = \frac{\left(S\, A_1\, A_2\right)^2}{\left(N_1\, A_1\, A_2\right)^2 + \left(N_2\, A_2\right)^2} \tag{3.7}$$

$$\left(\frac{S}{N}\right)^2 = \frac{S^2}{N_1^2 + \left(\frac{N_2}{A_1}\right)^2} = \left(\frac{S}{N_1}\right)^2 \left\{\frac{1}{1 + \left(\frac{N_2}{A_1\, N_1}\right)^2}\right\} \tag{3.8}$$

The noise contribution from the second-stage can be negligible, provided the gain of the first stage is sufficiently high in equation 3.8. Therefore in a well-designed system, the noise is dominated by the first gain stage [10].

3.5.4 Amplifier Noise Model

The noise properties of any amplifier can be described fully in terms of "voltage noise" and "current noise" sources at the amplifier input, with magnitudes ($\frac{V}{\sqrt{Hz}}$) and ($\frac{A}{\sqrt{Hz}}$). Figure 3.10 shows the noise model for op-amp.

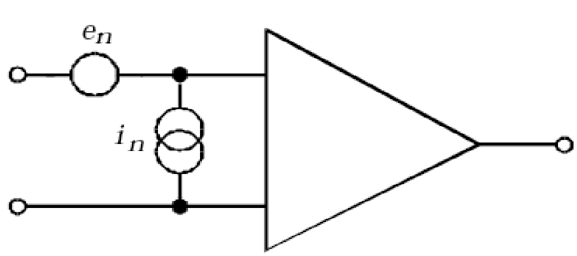

Figure 3.10 : Amplifier Noise Model

The magnitude of the noise sources are characterized by the spectral density. The noise sources don't necessarily have to be present at the input. Internal noise from the amplifier also contributes to the total noise.

Assume that at the output, the combined contribution of all internal noise sources has the spectral density e_{no}. If the amplifier has a voltage gain A_v, this means a voltage noise source at the input ;

$$e_n = \frac{e_{no}}{A_v} \quad \textbf{(3.9)}$$

Assume that a detector with resistance R_s is connected to an amplifier with voltage gain A_v and an infinite input resistance, so no current flows into the amplifier. Figure 3.11 shows the schematics.

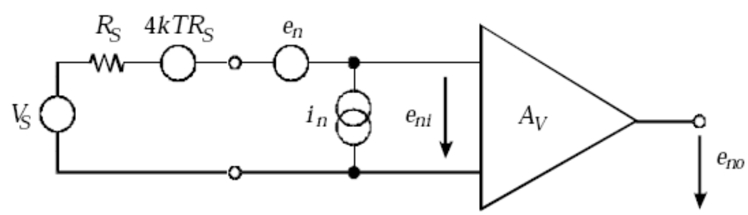

Figure 3.11 : Detector with Resistance R_s Connected to the Infinite Resistance

The input noise current flows through the source resistance R_s to yield a noise voltage ($I_n R_s$), which adds to the thermal noise of the source resistance and the noise voltage of the amplifier. Therefore the total noise voltage at the input of the amplifier is;

$$(e_{ni})^2 = 4kTR_s + e_n^2 + (I_n R_s)^2 \quad \textbf{(3.10)}$$

and at the output of the amplifier is;

$$(e_{no})^2 = (A_v e_{ni})^2 = A_v^2 \left[4kTR_s + e_n^2 + (I_n R_s)^2\right]^2 \quad \textbf{(3.11)}$$

and the signal to noise ratio at the amplifier's output is;

$$\left(\frac{S}{N}\right)^2 = \frac{V_s^2}{\left[4kTR_s + e_n^2 + (I_n R_s)^2\right]^2} \quad \textbf{(3.12)}$$

Because A_v^2 terms cancels theirselves, the S/N ratio of amplifier is independent of the amplifier gain and equal to the input S/N, because of both the input noise and the signal are amplified by the same amount. In the previous example, the amplifier had an infinite input resistance, so no current flowed into the amplifier. But now a finite input resistance is added as shown in Figure 3.12.

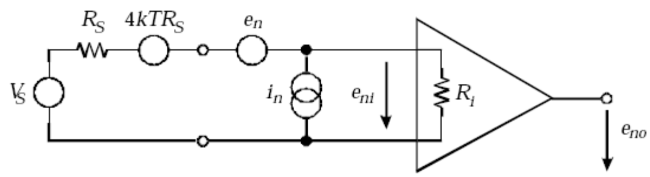

Figure 3.12 : Detector with Resistance R_s Connected to the Finite Input Resistance

The signal at the input of the amplifier is;

$$V_{si} = V_s \frac{R_i}{R_s + R_i} \tag{3.13}$$

The noise voltage at the input of the amplifier is;

$$e_{ni}^2 = \left[\left(4kTR_s + e_n^2\right) \left(\frac{R_i}{R_i + R_s} \right)^2 \right] + I_n^2 \left(\frac{R_i\, R_s}{R_i + R_s} \right)^2 \tag{3.14}$$

Note that the bracket near the I_n^2 term in equation 3.14 comes from the parallel combination of R_i and R_s. The signal to noise ratio at the output of the op-amp is;

$$\left(\frac{S}{N}\right)^2 = A_v^2 \frac{V_{si}^2}{A_v^2}\, e_{ni}^2 \tag{3.15}$$

$$\left(\frac{S}{N}\right)^2 = \frac{V_s^2 \left(\frac{R_i}{R_s + R_i} \right)^2}{\left(4kTR_s + e_n^2\right) \left(\frac{R_i}{R_i + R_s} \right)^2} + I_n^2 \left(R_i \frac{R_s}{R_i + R_s} \right)^2 \tag{3.16}$$

Note that equation 3.16 and equation 3.14 are the same. These results are also same for complex input impedance which is a combination of resistive and capacitive or inductive components [10]. So these results show that the S/N ratio is independent of the amplifier's input impedance.

3.5.5 S/N in Capacitive Signal Sources

Detector is a good example for a capacitive signal sources. Equivalent circuit for a classical detector-opamp system is shown in Figure 3.13.

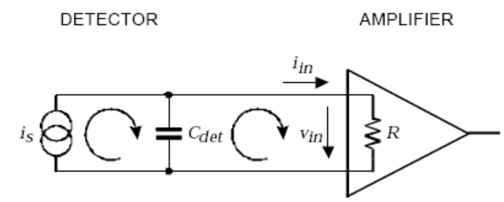

Figure 3.13 : Detector – Op-amp System

Note that the charges moving in detector induce change of charge on detector electrodes and the detector capacitance discharges into amplifier.

Assume an amplifier with constant noise. So the signal-to-noise ratio (and the equivalent noise charge) depends on the signal magnitude. Pulse shape which is registered by the amplifier depends on the input time constant $R.C_{det}$. Now assume a rectangular detector current pulse of duration T and magnitude I_s.

So if;

$0 \leq t < T$ $$I_n(t) = I_s\left[1 - \exp\left(-\frac{t}{RC}\right)\right] \tag{3.17}$$

$T \leq t \leq \infty$ $$I_n(t) = I_s\left[\exp\left(\frac{T}{RC}\right) - 1\right]\exp\left(-\frac{t}{RC}\right) \tag{3.18}$$

Where I_s = Shot Noise Current and I_n = Noise Current

This means at short time constants (RC<<T), the amplifier pulse approximately follows the detector current pulse. But as the input time constant RC increases, the amplifier signal becomes longer and the peak amplitude decreases as can be shown in Figure 3.14 and 3.15.

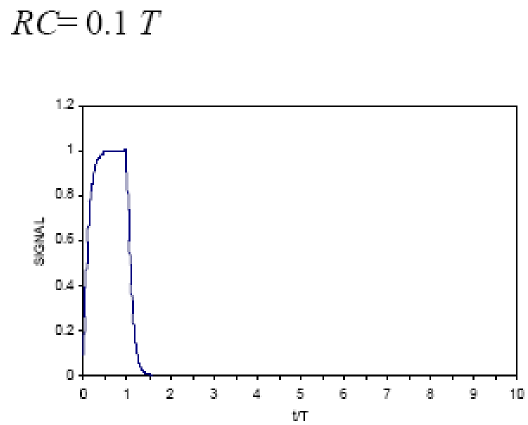

Figure 3.14 : Amplifier Signal for RC = 0,1T [10]

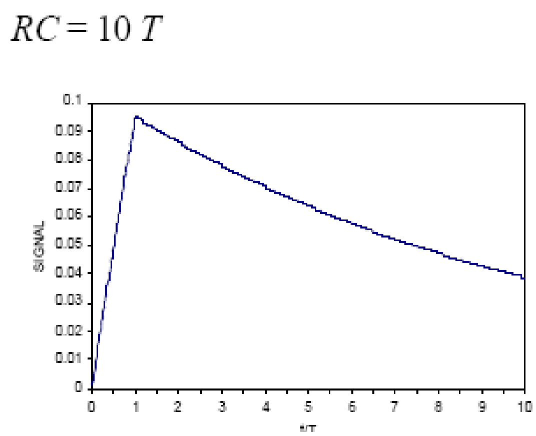

Figure 3.15 : Amplifier Signal for RC = 10T [10]

So at long time constants (RC>>T), the detector signal current is collected on the detector capacitance and the input voltage sensed by the amplifier is;

$$V_{in} = \frac{Q_{det}}{C} = \int_0^T \frac{I_s \cdot dt}{C} \qquad \textbf{(3.19)}$$

So it can be seen that the peak amplifier signal is inversely proportional to the total capacitance at the input which is the sum of detector capacitance, input capacitance of the amplifier, and the other capacitances [10].

But at small time constants the amplifier signal approximates the detector current pulse and it is independent of capacitances. At large input time constants (RC/T > 5) the maximum signal falls linearly with capacitance.

In a voltage-sensitive preamplifier;

-Noise voltage at the output is independent of the detector's capacitance. The equivalent input noise voltage is $V_{ni} = \frac{V_{no}}{A_v}$

-Input signal decreases with increasing input capacitance (equation 3.19), so signal to noise ratio depends on detector capacitance.

In a charge-sensitive preamplifier, the signal at the amplifier output is independent of detector capacitance (if $C_i >> C_{det}$).

-Noise appearing at the output of the preamplifier is fed back to the input, decreasing the output noise from the open-loop value $V_{ni} = \frac{V_{no}}{A_v}$.

-The magnitude of the feedback depends on the shunt impedance (ex: detector capacitance) at the input. Note that the dominant noise sources are typically internal amplifier noises. Only in a feedback configuration, some of this noise actually is present at the input. In other words, the primary noise signal is not a physical charge (or voltage) at the amplifier input, to which the loop responds in the same manner as to a detector signal. So, the S/N at the amplifier output depends on feedback.

4. OPERATION OF RADIATION DETECTORS

Radiation is defined as the process, in which energy is emitted as the particles or waves. Radiation depending on its effect on atomic matter can be classified as;

1- Ionizing Radiation

2- Non-Ionizing Radiation.

The most common use of the word "radiation" refers to ionizing radiation. Ionizing radiation has enough energy to ionize atoms or molecules while non-ionizing radiation does not.

Common types of radiation are; Gamma-Ray, Beta, Alpha, Neutron and X-Ray. Gammas and X-Rays are the part of electromagnetic radiation. It's especially interested in gamma-ray and X-ray radiations in this chapter.

Gamma radiation is a high-energy electromagnetic radiation emitted by certain radionuclides. Usually it happens after alpha or beta decays. The excess energy of the excited nuclei can be released by the transition of nuclei from a higher to a lower energy state. All gamma-rays emitted from a given isotope are characteristic and this enables scientists to identify which gamma emitters are present in a sample. The gamma energies can start from couple of keV to couple of MeV.

X-Ray radiation is electromagnetic radiation not emitted from the nucleus, but emitted by energy changes of atomic electrons. These energy changes are either in electron orbital shells that surround an atom or in the process of slowing down such as in an X-ray machine (Bremhstrahlung). Radioactive source based X-ray energies can start from couple of keV and extend up to 80 keV.

Radiation must interact with matter in order to be detected. The ionization process forms the basis for most detector systems. There's no single type of detector/detection scheme that can be equally useful for all types of radiations, because of the differences in the interaction mechanism with matter. In addition, radiation levels and energies to be detected vary drastically.

Activities can range from a few counts per hour up to 10^{13} count per second or more. The energies of common radiations can be as low as a fraction of an eV up to the GeV level. Therefore, there're many detector types appropriate for different type of radiations, energies and activities.

Detector systems are divided into two major groups;

1- Electronic Detection Systems: Operating principle of these systems is based on the electrical signals generated when radiation passes through the detector volume. These are the most common detection systems.

2- Other Detectors: These are the detectors which don't require the direct measurement of an electrical pulse or current. Some examples can be given as photographic plates, chemical reaction dosimeters, calorimetric dosimeters, cloud and bubble chambers and thermo luminescence detectors.

4.1 Gamma-Ray / X – Ray Interactions with Matter

Knowledge of gamma-ray interactions is important to the non-destructive analysis in order to understand gamma-ray detection and attenuation. A gamma-ray must interact with a detector in order to be "seen".

When a gamma-ray passes through the matter, the probability for absorption in a thin layer is proportional to the thickness of the layer. This leads to an exponential decrease of intensity with thickness which is formulated in equation 4.1.

$$I(x) = I_o \exp(-\mu x) \tag{4.1}$$

Here, $\mu = n.\sigma$ is the absorption coefficient, measured in cm^{-1}, n is the number of atoms per (cm^3) in the material, σ is the absorption cross section in (cm^2) and x is the thickness of material in (cm).

In passing through matter, gamma radiation ionizes via three main processes; the photoelectric effect, the Compton scattering, and the pair production.

4.1.1 The Photoelectric Effect

In the photoelectric effect, a gamma-ray interacts with an atom in a process which results the ejection of electron from the atom and the disappearance of the gamma-ray. The electron receives all the gamma-ray energy, minus its atomic binding energy.

The gamma energy is used for breaking the atomic binding and the rest of the energy is transferred to electron as kinetic energy. We can write the energy equation for a photoelectric effect using the conservation of energy as;

$$E_{pe} = E_{\gamma} - W = \frac{hc}{\lambda} \qquad \textbf{(4.2)}$$

Where W is the binding energy (or generally called as "work function"). The ejected electron can then induce (if there is enough kinetic energy) secondary ionization.

The probability of occurrence of the photoelectric effect is directly related to Z (atomic number) of the absorber and inversely related to the energy of gamma-ray.

$$P_{pe} = k \frac{\left(Z_{abs}\right)^{5}}{\left(E_{\gamma}\right)^{\frac{7}{2}}} \qquad \textbf{(4.3)}$$

Thus, photoelectric effect occurs most often for gammas which have relatively low gamma energy (< 1 MeV) in high-Z absorbers.

Laws of the photoelectric effect can be listed as;

1- For a given material as a target and frequency of incident radiation, the rate of ejection of photoelectrons is directly proportional to the intensity of the incident radiation.

2- For a given material, there exists a certain minimum frequency of incident radiation below which no photoelectrons can be emitted. This frequency is called the "threshold frequency".

3- Above the threshold frequency, the maximum kinetic energy of the emitted photoelectron is independent of the intensity of the incident radiation but depends on the frequency.

4- The time lag between the incidence of radiation and the emission of a photoelectron is very small, less than 10^{-9} seconds.

4.1.2 Compton Scattering

In the photoelectric effect, all gamma energy is lost in a single interaction with an atomic electron. A gamma-ray may also interact with an atomic electron in such a way that it loses only part of its energy. In this process, an electron is ejected away from the atom and it gains energy which is lost by the gamma.

The gamma-ray, which has now less energy, is deflected from its original path. This process is called "Compton Scattering". The scattered electron can cause second ionization events. Using the conversation of energy and momentum, Compton Scattering can be formulated as;

$$\lambda_{final} - \lambda_{initial} = h\,\frac{(1-\cos\theta)}{m_e\,c} \qquad \textbf{(4.4)}$$

The probability of Compton Scattering is directly related to the number of electrons in the atoms of the absorber material (and thus Z), and inversely related to the gamma energy;

$$P_{cs} = k\,\frac{Z_{abs}}{E_\gamma} \qquad \textbf{(4.5)}$$

Compton scattering mostly occurs for gamma-rays in the 0,6 – 4,0 MeV energy range in absorbers with high Z. Compton interactions will result in the production of a continuum of scattered gamma-ray energies down to minimum value. The minimum energy of a Compton scattered gamma-ray (or maximum energy of a Compton electron) would be the energy remaining after it was scattered at 180^0 from its original direction.

4.1.3 Pair Production

The third major mode of interaction of gamma-rays with matter is less common than the first two, and occurs only for high energy gamma-rays. Near the nucleus of an absorber atom, the gamma-ray is transformed to matter in the form of electron and positron. This event is called pair-production.

Because an electron has a rest mass equivalent to 0,511 MeV of energy, minimum gamma-ray energy of 1,022 MeV is required for this transformation to occur. If the incident gamma-ray has energy above 1,022 MeV, the rest of the energy is given to electron-positron pair as kinetic energy.

The pair production occurrence probability is related with the gamma energy and the Z of the absorber. It's given by the equation 4.6

$$P_{pp} = k \, \text{Log}\left(E_{\gamma}\right)\left(Z_{abs}\right)^{2} \qquad \textbf{(4.6)}$$

Generally, the created positron will slow down in the absorber and undergo annihilation producing two 0,511 MeV photons. These two gamma-rays may or may not reabsorb in the detector material. If only one of them is absorbed in the detector material, it is called as "single escape". If none of them is absorbed then it is called as "double escape".

4.2 Definition of Detector Operating Characteristics

There are three parameters that are generally used in characterizing the various types of detectors. They are efficiency, resolution and dead time or resolving time of the detector.

4.2.1 Efficiency of a Detector

Efficiency of a detector is defined as the number of radiations actually detected out of the number emitted by the source. There are two ways to define the efficiency. One is based on the number of radiations emitted by the source (Absolute Efficiency) and the other is based on the number of radiations that strike the detector (Intrinsic Efficiency) which are;

ε_{abs} = Number of pulses recorded / Number of radiations emitted by the source.

ε_{int} = Number of pulses recorded / Number of radiations stroked to the detector.

Mostly, high efficiency is desired. For non-penetrating radiations, such as heavy charged particles, 100% efficiency can be reached but for the more penetrating uncharged radiations (such as X and gamma), detection efficiency will generally be much lower.

Detector efficiency depends upon;

1- The detector size and shape (where larger areas and larger volumes are more sensitive).

2- The distance from the detector to the radioactive material.

3- The radioisotope and the type of the radiation measured (alpha, beta, gamma radiation and their energies)

4- The backscattering of the radiation from the detector or detector window (Backscattering increases as the density of the backscatter material increases.)

5- The absorption of the radiation before it reaches the detector (by air and by the detector cover, etc…)

There are also many factors that effect detector efficiency. For example; some radiation go directly from the radioactive material into the detector, some radiation may scatter from the surface of the source or from the source holder. In this case detected energy of the radiation will be smaller. Some radiation may also be absorbed by the detector window.

4.2.2 Energy Resolution of a Detector

Energy resolution refers to the ability of the discrimination between two radiations of close energies. Not of all detectors can give energy information, so for these detectors this parameter is not defined.

Resolution is defined with reference to a plot of the number of radiations detected against certain radiation energy as follows;

$$R = \frac{\Delta E}{E_o} \tag{4.7}$$

Here E_0 is the energy corresponding to the center of the photo-peak and ΔE is the width of the peak halfway between the baseline and the top of the peak. ΔE is also called as the "Full Width at Half Maximum" or generally "FWHM" which can be seen in Figure 4.1. The resolution is often expressed as a percentage.

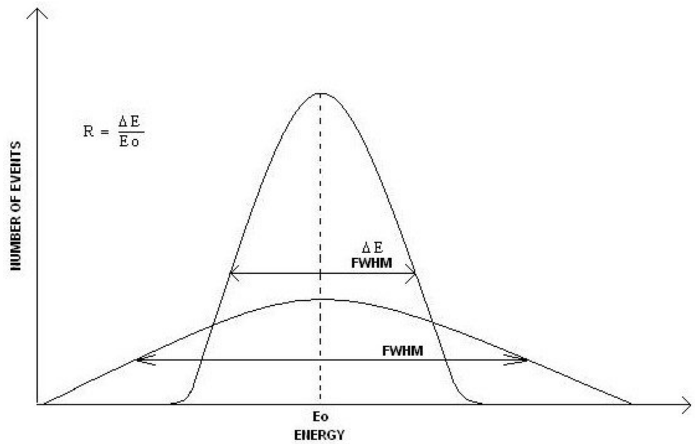

Figure 4.1 : Representation of Different Energy Resolutions[1]

The detectors that have the smaller value for resolution can separate two radiations of similar energy better. Resolution can not be perfect because of the electronic noise and the statistical nature of the interactions of radiation with matter. Resolution can vary greatly between different type detectors.

4.2.3 Dead (Resolving) Time of the Detector

Dead time means the amount of time needed before the detector can recover from one incoming radiation and respond to the next one. The total dead time of a detection system is generally related to the contributions of the intrinsic dead time of the detector (Ex : the drift time in a gaseous ionization detector), of the analog front end and of the DAQ (the conversion time of the ADC's, the readout and storage times).

The intrinsic dead time of a detector is often related to its physical characteristic (for example; a spark chamber is "dead" until the potential between the plates recovers above a high enough value). In other cases the detector is still "live" and produces a signal for the successive event, but the signal is such that the detector readout is unable to discriminate and separate them resulting an event loss or in a so called "pile-up" event where, for example, a sum of the deposited energies from the two events is recorded instead. In some cases this can be minimized by an appropriate design, but often this can cause the loss of other properties like energy resolution.

A detector, or a detection system, can be characterized by a paralizable or nonparalizable behavior.

In a non-paralizable detector, an event happening during the dead time since the previous event is simply lost, so that with an increasing event rate the detector will reach a saturation rate equal to the inverse of the dead time.

In a paralizable detector, an event happening during the dead time since the previous one will not just be missed, but will restart the dead time, so that with increasing rate the detector will reach a saturation point where it will be incapable of recording any event at all.

A semi-paralizable detector shows an intermediate behavior, in which the event arriving during dead time does extend it, but not by the full amount, resulting in a detection rate that decreases when the event rate approaches saturation. Very fast detection systems may be able to respond to an event within nanoseconds.

4.3 Types of the Radiation Detectors

Electronic radiation detectors can be grouped as;

- Gas-Filled Detectors
  - Ionization Chambers
  - Proportional Counters
  - Geiger Counters
- Solid-State Detectors
  - Scintillation Detectors
  - Semiconductor Detectors

4.3.1 Gas-Filled Detectors

Gas filled detectors consist of a volume of gas surrounded by a housing that may either be sealed or designed to permit a continuous flow. There are electrodes within the gas volume and voltage is applied between electrodes which creates an electric field. When radiation passes through the gas filled area, it ionizes the gas molecules to form ion pairs (electron and positive ion). Generated ions are pulled to the electrodes and this produces the electrical signal that indicates the existence of radiation.

The electrical signal to be measured may either be a current, a voltage pulse or a total accumulated charge depending on the design of the detector. The energy lost by the incoming radiation to form an ion pair in the gas is about 30-35 eV where the actual value can vary by a few eV depending on the gas.

Three kinds of gas filled detectors will be discussed here. Ionization chamber, proportional counters and Geiger-Muller counters which differ primarily in the strength of the electric field applied across the electrodes.

A graph showing the relationships of the output signal (ion pairs collected) of a gas filled counter to the applied voltage is shown in Figure 4.2. Curves for sources undergoing decay via single α-, β- or γ-particle transitions are illustrated.

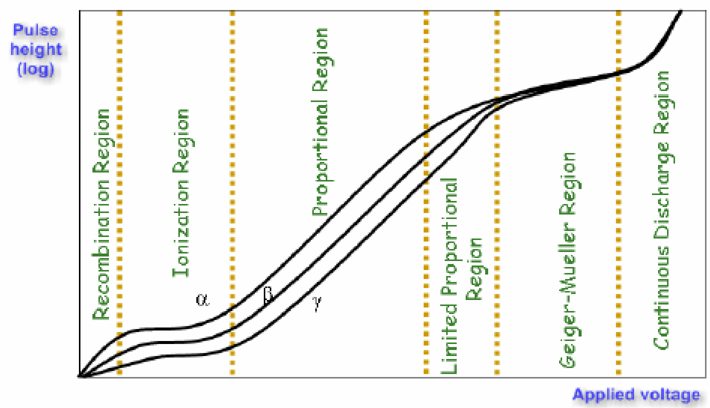

Figure 4.2 : Applied Voltage versus Collected Ion Pairs[1]

In the recombination region, voltage is too low for all the ion pairs to be collected. Many of the ions may simply recombine. So this region is not useful for detection. In ionization region, voltage is high enough to collect all the ion pairs formed by a single ionization. However the ions are not accelerated enough to produce second ionization. So the amplitude of the produced signal is related to the incoming photon energy. This is the region where ionization chamber works.

At higher voltages, in the proportional region, the electrons formed by incoming photon are accelerated enough to have kinetic energy that can induce secondary ionization.

The amplitude of the signal is not constant with changing detector voltage but it is still linearly depend on the incoming photon energy. This is the region of the operation for proportional counters.

With the increasing detector voltage, in the limited proportional region, the linear relationship between the energy of incoming photon and the produced ions begins to be spoiled. So this region is not useful for detection. In the G-M region the voltage is so high that the single ionizing can cause the electrical discharge of the entire tube. The G-M counter is operated in this region. Because only a single amplitude signal is produced by any incoming radiation, the energy discrimination is not available for G-M counters.

At very high voltages, continuous discharge occurs in the gas and this region is not useful for detection.

4.3.1.1 Ionization Chambers

Ionization chamber is one of the simplest and the oldest radiation detector. The chamber is typically a few centimeters in diameter filled with a gas at pressure ranging from 0,1 – 10 Atm. A simple diagram for ionization chamber is shown in Figure 4.3.

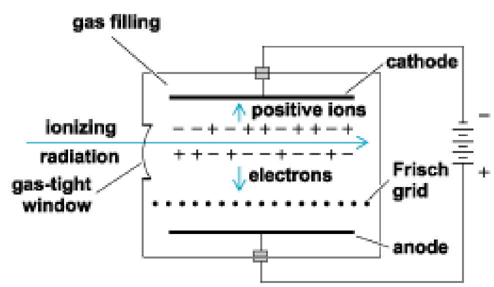

Figure 4.3 : Ionization Chamber[1]

When the radiation passes through the chamber, ion pairs are formed. If there is no electric field present, ion pairs will simply recombine. But if a large enough electric field is applied between the plates, then the ions will drift toward the electrodes. The measured electrical signals may either be a current, a voltage pulse or the accumulation of the total amount of charge depending on the design of electrical circuit used.

One of the most important uses of an ionization chamber is to measure the total energy of a particle, or the energy lost in case the particle does not stop in the chamber. In addition to give energy information, ionization chambers are now built to give information about the position of the incoming radiation within the gas volume where the initial ionization event occurred.

This information can be important not only in experiments in nuclear and high-energy physics where these position sensitive detectors were first developed, but also in medical and industrial applications.

4.3.1.2 Proportional Counters

Proportional counters are gas filled detectors that is operated in higher voltages than the ionization chambers. A proportional counter is shown in Figure 4.4.

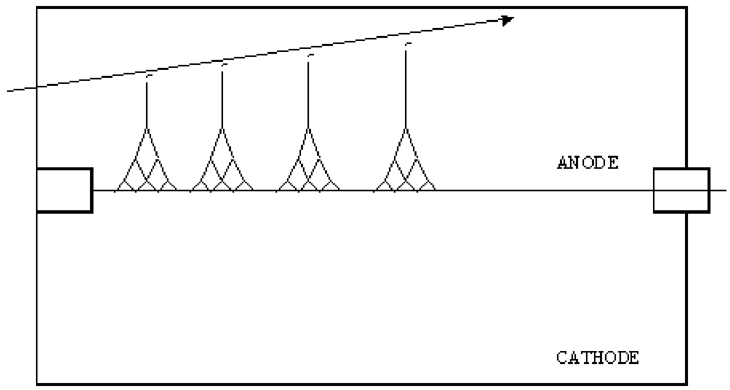

Figure 4.4 : Proportional Counter

Because of the higher electric field, the ion pair generated by the incoming radiation is accelerated to a greater velocity when they drift toward the electrodes. The increase in the kinetic energy means the collisions between the electrons and other gas molecules are energetic enough to induce secondary ionization with the release of more free electrons which means the internal multiplication of original signal occurs. This multiplication process is called “Townsend Avalanche”. If conditions are proper the signal amplification can be kept linearly proportional to the original number of ion pairs generated. Therefore energy information is retained.

If the voltage is lowered below a critical value, the electrons do not gain sufficient kinetic energy as they drift to create second ionization, so the detector operates as an ionization chamber. If the voltage is too high, the degree of charge amplification tends to a maximum value, and all pulses from the chamber have the same amplitude, so the detector operates as a Geiger-Muller counter.

4.3.1.3 Geiger Muller Counters

The third type of gas-filled detector is the Geiger-Muller (G-M) counter. These are the most used detector types when gross activity level is primary interest. In G-M counters, applied voltage is higher compared to ionization chambers and proportional counters. A Geiger-Muller counter is illustrated in Figure 4.5.

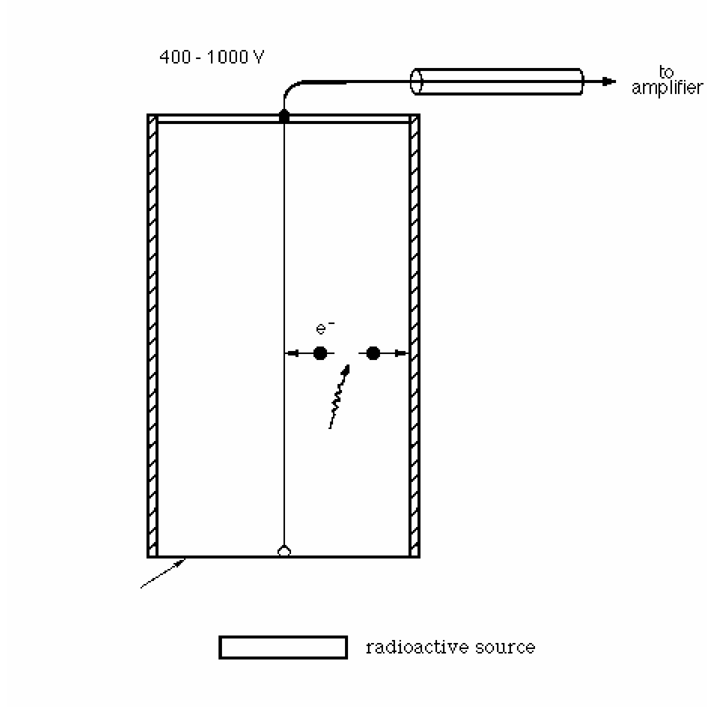

Figure 4.5 : Geiger-Muller Tube

As a result of stronger electric field, the electrons created are accelerated strongly towards the anode and are gained high kinetic energies. The electrons can induce second ionization as they do in proportional counters. However in GM tube, greater energy and larger number of collisions result in the excitation of many gas molecules, some of them will de-excite by emission of energetic photons. These photons can cause new ionizations in the tube which results a propagated Townsend avalanche spreads around the entire anode of the detector.

The Geiger-Muller counter is used for detecting and measuring low level β-particle and γ-ray radiation. It cannot detect α-particles. A "Geiger counter" usually contains a metal tube with a thin metal wire along its central-axis. The space in between them is sealed off and filled with a suitable gas. The wire is hold about at +1000 volts relative to the tube.

4.3.2 Solid-State Detectors

There is a class of detectors known as solid-state detectors which work on the principle that they collect the charge generated by ionizing radiation in a solid. These detectors are made of semi-conducting material and are operated much like a solid-state diode with a reverse bias. The applied high voltage generates a thick depletion layer and any charge created by the radiation in this layer is collected at the electrode. The charge collected is proportional to the energy deposited in the detector and therefore these devices can also give information about the energy of individual particles or photons of radiation. The detectors are made mostly from silicon or germanium.

4.3.2.1 Scintillation Detectors

The basic function of a scintillation detector, much like other types of detectors, is to transform the energy of an incoming particle to a measurable electronic signal. A scintillation detector consists of two components:

1. Scintillator
2. Photomultiplier or PIN diode

The scintillator converts a fraction of the energy of the incoming particle to light and the photomultiplier tube (PMT) converts the light to a current signal, which can be manipulated in the electronics system.

The scintillation detector is one of the most common detector devices used in nuclear and particle physics experiments as well as in nuclear medicine.

The general description of a scintillator is a material that emits low-energy (usually in the visible range) photons when struck by a high-energy charged particle. When used as a gamma-ray detector, the scintillator does not directly detect the gamma-rays. Instead, when a particle passes through the scintillating material, it collides with atomic electrons, exciting them to higher energy levels. After a very short period of time, the electrons fall back to their natural levels, causing emission of light.

There are six different types of scintillators:

1. Organic crystals
2. Organic liquids
3. Plastics
4. Inorganic crystals
5. Gases
6. Glasses

For heavy-ion detection the inorganic crystals provide by far the best characteristics. Furthermore, these groups of scintillators together with the glasses are the most suitable.

A photomultiplier is a device that converts visible light to electric current. It consists of three parts [12]:

1. Photocathode,
2. Electron-Multiplier section,
3. Anode.

In the photocathode an incident photon is absorbed by photoelectric effect, releasing an electron. In the Electron-Multiplier section this electron is accelerated through a series of secondary emission electrodes, dynodes, knocking out a number of new electrons from each of them, multiplying the number of electrons in each step. After multiplication, the total electron current is collected in the anode. In a typical PMT, the multiplication factor is in the order of 10^7 which means a single electron is multiplied with 10^7 electrons. A typical photomultiplier tube is shown in Figure 4.6.

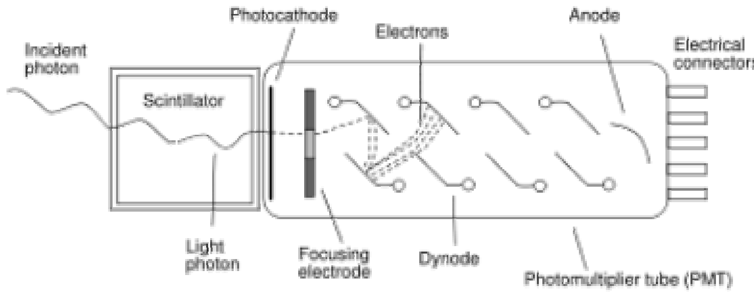

Figure 4.6 : Photomultiplier Tube[1]

4.3.2.2 Semiconductor Detectors

In these detectors, radiation is measured by the number of charge carriers set free by the incoming radiation in the detector, which is arranged between two electrodes. Ionizing radiation produces free electrons and holes. The number of electron-hole pairs is proportional to the energy transmitted by the radiation to the semiconductor. As a result, a number of electrons are transferred from the valence band to the conduction band, and an equal number of holes are created in the valence band. Under the effect of an electric field, electrons and holes travel to the electrodes, where they result in a pulse that can be measured in an outer electronic circuit. The holes travel into the opposite direction and can also be measured. The amount of energy required to create an electron-hole pair is known, and is independent of the energy of the incident radiation, measuring the number of electron-hole pairs allows the energy of the incident radiation to be found.

The energy required for production of electron-hole-pairs is almost 10 times smaller in solid-state detectors compared to the one in gaseous detectors. Consequently, in semiconductor detectors the statistical variation of the pulse height is smaller and the energy resolution is higher. As the electrons travel fast, the time resolution is also very good and is dependent upon rise time. Compared with gaseous ionization detectors, the density of a semiconductor detector is very high, and charged particles of high energy can give off their energy in a semiconductor of relatively small dimensions.

4.4 Electronic Components of the Detectors

Electronic detectors are based on the voltage pulse measurement that requires many other electronic components. All of the detectors that are discussed need application of a voltage, generally called “detector bias”. Therefore a high voltage supply or “detector bias supply” is the essential component of the electronic counter system. This voltage supply must be able to give a range of stable DC voltage to meet the requirements of the different types of detectors.

A preamplifier is needed for the detectors that generate pulses at small amplitudes. Preamplifier should be located very close to the detector to avoid loss of signals and interferences. This device serves for maximizing the signal to noise ratio from the detector and provides first amplification and pulse shaping of the small signals coming out of detector. The amplifier section accepts the pulses coming from the preamplifier and amplifies them further more. It also shapes the pulses for improved processing of the signal by the signal processing and data storage system. The amplitude of the signals coming out of the amplifier is related to the energy of the radiation which produces these pulses. A block diagram for an electronic detector is shown in Figure 4.7.

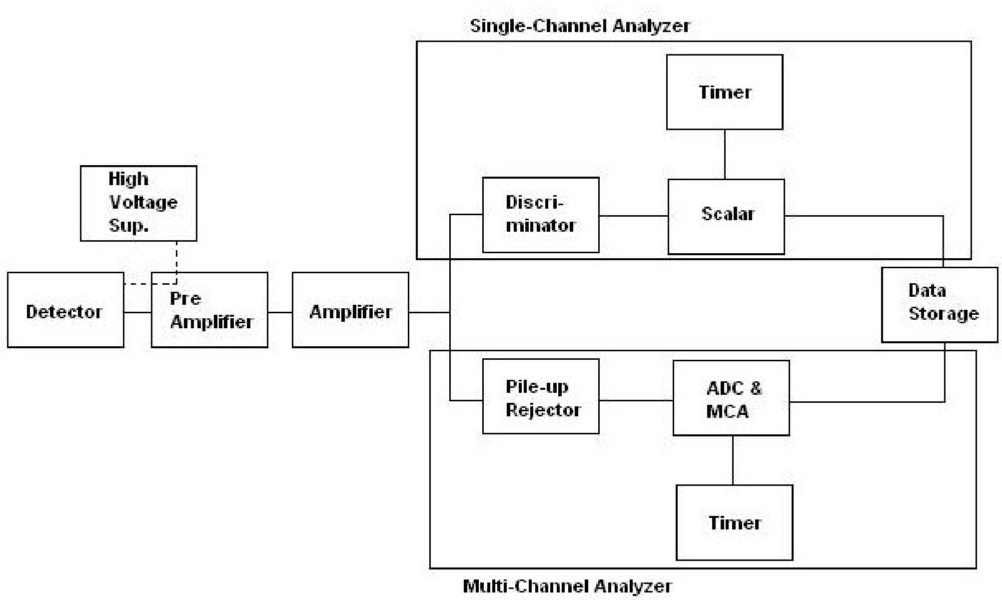

Figure 4.7 : Block Diagram of a High Resolution Radiation Detection System

When the radiations of more than one energy strikes the detector, pulses at different amplitude will be produced.

If only one of the particular radiation energy is interested, the pulses that correspond to interested energy can be selected with a device named “discriminator”. This is the electronic device that can be set to accept only pulses above or between preset amplitudes. A lower level discriminator (LLD) sets the lower amplitude limit while an upper level discriminator (ULD) sets the upper limits. This can be shown in Figure 4.8.

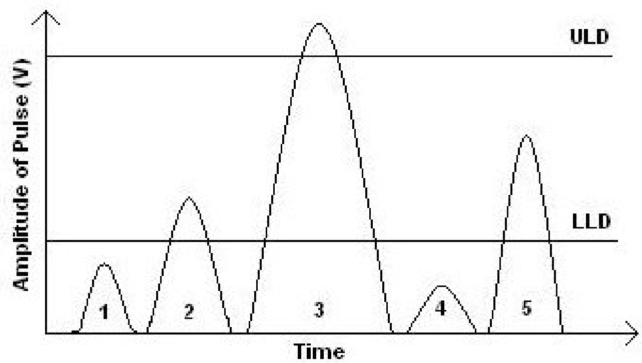

Figure 4.8 : Utilization of a Single Channel Analyzer for Energy Discrimination

For example, pulse 2 and 5 are the signals that will be accepted and pulse 3 will be rejected by the system. A simple discrimination device that allows both the LLD and the ULD to be preset is called a SCA (Single Channel Analyzer).

The Multichannel Analyzer (MCA) can be considered as a series of SCA’s with incrementing narrow windows. It consists of an Analog to Digital Converter (ADC), control logic, memory and display. The MCA collects pulses in all voltage ranges at once and displays this information in real time, providing a major improvement over SCA spectrum analysis. Multichannel analyzer can scan a whole energy range and record the number of pulses they count in each of the channels.

5. EXPERIMENTAL SECTION – INTRODUCTION TO THE DETECTOR CIRCUIT

5.1 Gamma-Ray and Silicon Substance Interactions

In the test of the detectors, we used standard gamma-ray sources. The most used sources were Cs-137, Am-241 and Co-60. Gamma-rays from these sources cover a range of energies from 60 keV to 1332 keV.

Am-241 emits gamma-rays at 60 keV where Cs-137 emits gamma-rays at 662 keV. Let's assume both of these standard sources have an activity of 10 μCi. It can be calculated from the equation 5.1 how much photo-current is induced in Hamamatsu S1223-01 silicon PIN photodiode due to the incoming photons at these energies.

$$I = N.e.\varepsilon.E_{avg}.A / s \qquad \textbf{(5.1)}$$

Note that for Silicon, ionization constant (energy required to create one electron-hole pair) is only 3,6 eV [13]. The detection efficiency is a function of the thickness of the silicon wafer in the photodiode. For a wafer thickness of 300 μm (ignoring attenuation in the diode window and/or package), the detection efficiency is close to 100% at 10 keV and falling to approximately 1% at 150 keV [14]. For energies above approximately 60 keV, photons interact almost entirely through Compton scattering. Moreover, the active region of the photodiode is in electronic equilibrium with the surrounding medium (the diode package, substrate, window and outer coating), so that Compton electrons that are produced close to the active volume of the photodiode are also detected. For this reason the overall detection efficiency at 150 keV and above is maintained fairly constant (approximately 1%) over a wide range of photon energies. In the preceding calculation, the detection efficiency is taken 0,01 for Cs-137 and 0,02 for Am-241. The determination of the relative efficiency between the 60 keV and the 662 keV is going to be given in the next chapter.

The calculation of the current induced by 662 keV gamma of Cs-137 is as follows. First, we have to calculate the gamma-ray flux on the detector and average energy of the electrons. From Compton scattering, maximum energy of electrons is determined from the case where incoming photon is backscattered (θ=180) as in equation 5.2. This leads maximum energy deposition to the crystal structure from the incoming photon.

Maximum energy;

$$E_{max} = E_{\gamma}\left[\frac{2\,E_{\gamma}}{m_e c^2 + 2\,E_{\gamma}}\right] \tag{5.2}$$

For 662 keV;

$$E_{max} = \frac{2 \times 662^2}{511 + 2 \times 662} = 448\ \text{keV}.$$

For average energy;

$$E_{av} = \frac{E_{max}}{2} = 224\ \text{keV} \tag{5.3}$$

Also assuming gamma-rays are distributed isotropically from the source, gamma-ray flux at r distance from the source is;

$$N = \frac{A_s}{4\pi\, r^2} \tag{5.4}$$

Here A_s is the activity of the source and r is the detector source distance where it is taken as 1 cm for this calculation. Therefore count rate on the detector surface is:

$$N = \frac{10.10^{-6}\ 3{,}7\,10^{10}}{4\pi\, 1^2} = 29444\left(\frac{\gamma}{cm^2 \cdot s}\right)$$

Hence using the equation 5.1, we end up with;

$$I = (29444) \times \left(1{,}6 \times 10^{-19}\right) \times \left(0{,}01\right) \times (224000) \times \frac{0{,}13}{3{,}6} = 0{,}38\ \text{pA}.$$

Note that Cs-137 gamma line at 662 keV produces photodiode current is 0,38 pA.

If we repeat the same calculation for Am-241, we find maximum and average energies as 11,4 keV and 5,7 keV respectively. Using the same gamma-ray flux from the equation 5.1, we find induce photocurrent from a 60 keV gamma as 0,04 pA.

As a result of this calculation, one can see both of these gamma interactions with silicon substance, produces very small current and proper amplification is needed.

5.2 Transimpedance Amplifier Stage

Photodiodes may be called into action for applications such as precision light meters, high-speed fiber-optic receivers. If it’s needed to amplify the photodiode current, the current must be first converted to a voltage. The op-amp’s transimpedance amplifier is shown in Figure 5.1.

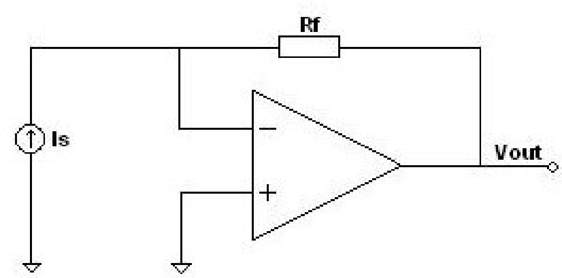

Figure 5.1 : Transimpedance Amplifier

The op-amp transimpedance amplifier (or current-to-voltage converter) is a fairly simple circuit. The feedback resistor R_f is connected between the output and the negative input. When some input current or photodiode current I_{in} flows through the negative input that is also known as the summing point, all of the current must go through the feedback resistor since the gain is so high (remember, no current flows into the op amp itself).

So, the output will be $V_{out} = I_n . R_f$ which means the input current is transformed to a voltage. That’s why this circuit is also called a "current-to-voltage converter" where the "gain" or "transimpedance" is equal to R_f.

There is a whole class of applications in which this configuration is quite useful and important. An important case is when op-amp is used to amplify the signal from a sensor, such as a photodiode. Photodiodes put out current at high impedance (high at DC), but often they have a lot of capacitance. If the photodiode current is just flow into a resistor, there are two problems.

If the resistor is large, then the gain can be fairly large. On the other hand, the response time, with the time-constant of $\tau = R.C_S$, where C_s is the photodiode capacitance, will be fairly large. But if a small resistor is chosen to get a small τ, then the gain will be low. The signal-to-noise ratio may also be unacceptable in this case. To avoid this, it is a good idea to feed the current output of the photodiode directly into the summing point of a transimpedance amplifier. Here, the response time is not $R_f.C_s$, but considerably faster. Moreover, the gain can be considerably larger, because larger R_F can be used now. This configuration helps to improve the signal-to-noise ratio too.

When the photodiode was connected up like in Figure 5.2, the observation was an oscillating output. The photodiode's capacitance C_S brings two negative effects into the circuit.

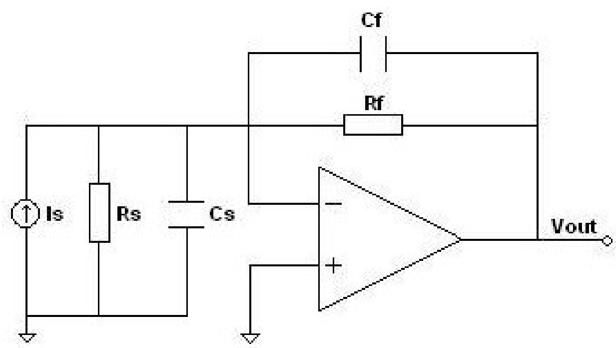

Figure 5.2 : Photodiode Connected to the Transempedance Amplifier

The first one is C_s tends to make circuit unstable and makes oscillation as the photodiode current runs along the feedback path from output to input, R_f and C_s create an RC circuit (low-pass filter) that cause oscillations at the output. The filters of the low-pass kind contribute negative phase to the feedback loop, making the circuit less stable. The second negative effect is C_s effectively places a short circuit across I_{in} at high frequencies, limiting the circuit's bandwidth.

Restoring stability requires destroying the effects of the undesirable low-pass filter constructed by R_f and C_s. It can be done with a construction of a high-pass filter in the same feedback path. So it's needed to add a feedback capacitor C_f across R_f to make it stable as shown in Figure 5.2. High-pass filter, constructed by C_f and R_s, adds positive phase to the loop pushing the circuit toward stability.

The formula for the optimized amount of C_f where GBW represents the gain bandwidth is;

$$\text{If } \left(\frac{R_f}{R_{in}}\right) \geq 2\sqrt{GBW\, R_f\, C_s} \qquad \text{Then} \quad C_f = \frac{C_s}{2\left(\frac{R_f}{R_{in}}+1\right)} \tag{5.5}$$

$$\text{But if } \left(\frac{R_f}{R_{in}}\right) < 2\sqrt{GBW\, R_f\, C_s} \qquad \text{Then} \quad C_f = \sqrt{\frac{C_s}{GBW\ R_f}} \tag{5.6}$$

Transimpedance amplifier stage is the first and most important part of the detector circuit. The photo-current signals coming from the photodiode and noise coming from both the photodiode and anywhere on the signal path are amplified together here. The noise sources on this path are; leakage current coming from the bias, the input current noise of the amplifier, resistors on the signal path and also noise contribution from the feedback capacitor. The noise factor here comes from the op amp's input-voltage noise is multiplied by the total capacitance at the op amp's inverting node. That capacitance includes the PIN photodiode capacitance, the input capacitance of the op-amp, and the feedback capacitance C_f. Thus; change in the feedback capacitor C_f will affect the noise level of the circuit. The transimpedance amplifier optimization is made and will be mentioned in the next chapter.

5.3 Shaping Amplifier Stage

Shaping amplifier stage is the part of our detector that the signals coming from the transimpedance amplifier are shaped. It's also called "pulse shaper". Shaping amplifier stage of our detector can be seen in Figure 5.3

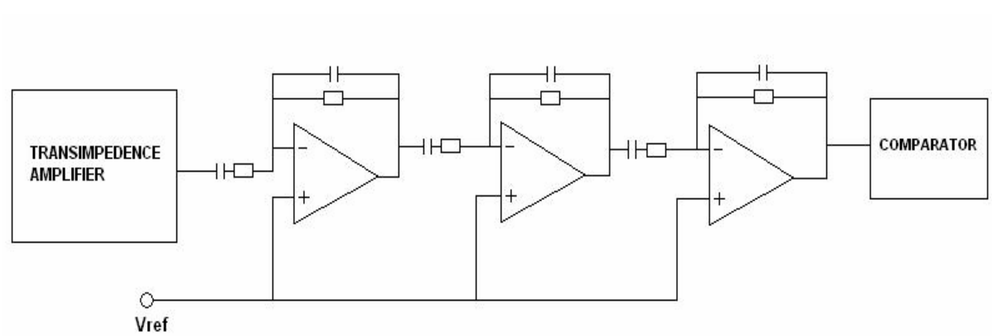

Figure 5.3 : Shaping Amplifier Stage

In the shaping amplifier stage there are two objectives; to improve S/N ratio and to improve pulse pair resolution. Increasing the pulse width helps to improve the S/N ratio where decreasing the pulse width helps to improve pulse pair resolution.

When increasing the pulse width; typically, the pulse shaper transforms a narrow detector signal pulse to a broader pulse for reducing the electronic noise. This transformed signal should have a gradually rounded maximum at the peaking time Tp (time needed for the peak to reach its maximum). If the shape of the pulse doesn't change with signal level, the peak amplitude is also a measure of the energy. So the pulse height spectrum is the energy spectrum.

Decreasing the pulse width is necessary for discriminating the pile-up signals. For example reducing the pulse shaping time to 1/3 generally eliminates pile-up. So it's important to find balance between these conflicting requirements. Sometimes minimum noise, sometimes rate capability is paramount. So the optimum shaping depends on the application.

In our design three shapers are connected in series. Additional shapers will give different output signals. It can be shown in Figure 5.4.

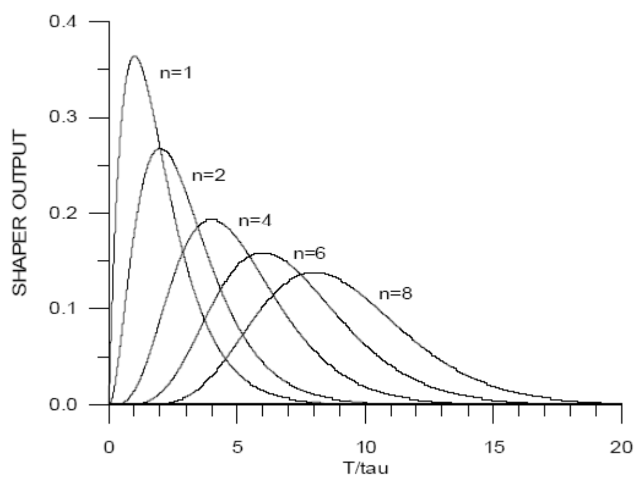

Figure 5.4 : Effect of the Additional Shapers in Signal Output [10]

In this figure, n is the number of the shapers used. The time constant of the shapers τ is chosen to be the same for all. As can be shown, additional shapers will change the peaking time T_p where $T_p = n.\tau$. Time constants can also be arranged for keeping T_p unchanged. They can be arranged as T(n) = T(n+1)/n that gives the outputs as in Figure 5.5.

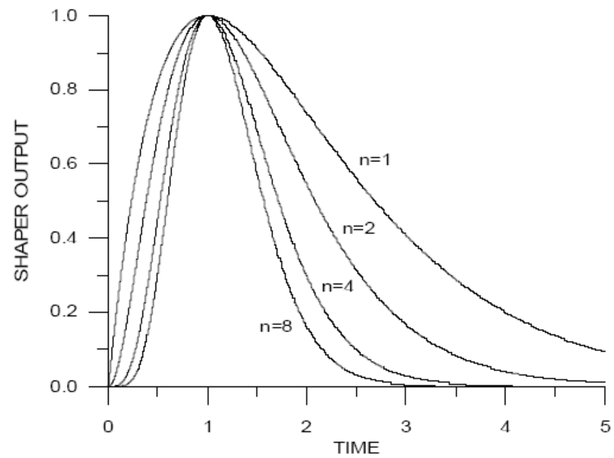

Figure 5.5 : Time Constant of Each Shaper is Arranged so T_p Remains Same [10]

So increasing the number of shapers makes the output pulse more symmetrical with a faster return to baseline. It also gives chance to improve rate capability at the same peaking time.

5.4 Selection Criteria

Selection of the suitable circuit elements is another important point of the detector circuit design. The best optimum selection for the used devices will give the best performance for the detector circuit. The most important parts of the detector circuit are the photodiode and the op-amp.

5.4.1 Photodiode Selection Criteria

One of the most critical parts of the detector circuit is the PIN Photodiode. The most critical parameters considered for photodiode selection are the sensitivity and the capacitance of the photodiode. The sensitivity (the number of the photons detected for a given radiation field) depends on the size of the depletion region of the photodiode. This means, the sensitivity depends on the area of the photodiode and the applied bias voltage. Hence, for maximizing the sensitivity, large area photodiodes with large bias voltage should be used. On the other hand, as the area of the photodiode gets larger, photodiode capacitance increases. This increases the noise level of the circuit. Also application of large bias voltage causes higher leakage current that also adds more to noise. In the presence of these, an optimal selection between the sensitivity and the capacitance should be made.

First, ordinary LEDs (Light Emitting Diode) were used instead of photodiodes. Visible light (sunlight, light coming from other LEDs) could be detected nicely, but no gamma detection was observed using LEDs as receiver. The sensitivity of the ordinary LEDs is not enough for gamma-ray detection. Another reason is no large bias voltage can be applied to ordinary LEDs and their active area is very small. Some of the phototransistors (Siemens BP103, Everlight PT331C, Fairchild QSD 124) were also tested instead of photodiodes and no gamma detection was observed neither. After all of these experiences and knowing Si PIN photodiodes are also used for medical imaging purposes [15], we decided to use them. The parameters of PIN photodiodes considered for our purpose are shown in table 5.1.

Table 5.1: Some Parameters of the Considered Photodiodes

Photodiode	Capacitance (pF)	Active Area (mm^2)	Spectral Sensitivity (A/W)	Max. Bias Reverse Voltage (V)
Hamamatsu S1223-01	20	12,96	0,6	30
Siemens BPW 33	630	7,34	0,59	7
Optec OP999	4	-	0,4	60
Fairchild QSE773	20	2,71	0,6	32
NEC PH302	14	9	0,6	32
Hamamatsu S875-16R	-	25	-	-

After several experiments made, gamma detection was observed with Hamamatsu S1223-01, Siemens BPW33 and Hamamatsu S 875-16R. The most optimal selection is seemed to be the Hamamatsu S1223-01 because of it has large active area and suitable capacitance. Some pictures of the Hamamatsu S1223-01 photodiode are given in Figure 5.6. As seen in this table, not all of the parameters were able to found from the literature.

Figure 5.6 : Some pictures of the Hamamatsu S1223-01 Photodiode

Some of the characteristics of the Hamamatsu S1223-01 photodiode taken from its datasheet are given below in Figure 5.7.

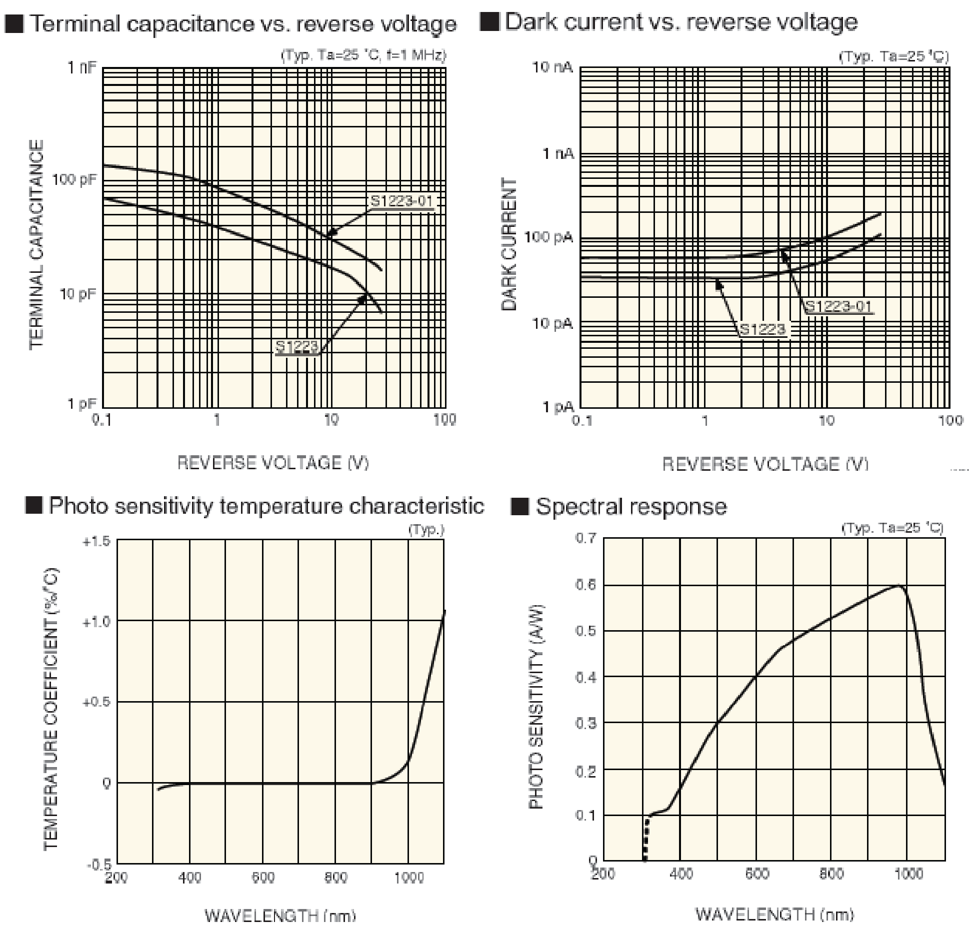

Figure 5.7 : Some Characteristics of the Hamamatsu S1223-01 Photodiode[16]

In Figure 5.7, the terminal capacitance of the photodiode is approximately 10 pF at the operating in reverse bias voltage of 30 V. Dark current begins to rise after 2 V reverse bias voltage. Photosensitivity has a maximum at the wavelength of 960 nm.

It's also tried to connect three BPW33 parallel to each other. This combination is increased the terminal capacitance and decreased the terminal resistance as expected. We observed a comparable count rate for Cs-137 in this setup. However no gamma-ray was observed for Am-241 for a photodiode BPW33.

5.4.2 Op-Amp Selection Criteria

Another critical part of the detector circuit is the op-amp. For the first stage of the amplification, the parameters of input-voltage noise, input-current noise, and the input capacitance of the op-amp must be considered seriously. All of these factors are effectively related with the noise level of the circuit. For example input-current noise of the op-amp is directly on the signal path and it's amplified along with the photo-signal. For that reason, the most important selection criteria for the op-amp is to have low input-current noise especially for the photoconductive type of connection. Also the input capacitance of the op-amp should be smaller compared to the terminal capacitance of the photodiode.

Of course there are many types of op-amps in the market. Many semiconductor manufacturers provide parametric search in their web sites. This helps end-user to choose the best integrated circuit to meet his design requirements. National Semiconductor provides a software called Selguide [17]. This software can be downloaded from their web site. The graphical user interface of the Selguide program can be seen in Figure 5.8.

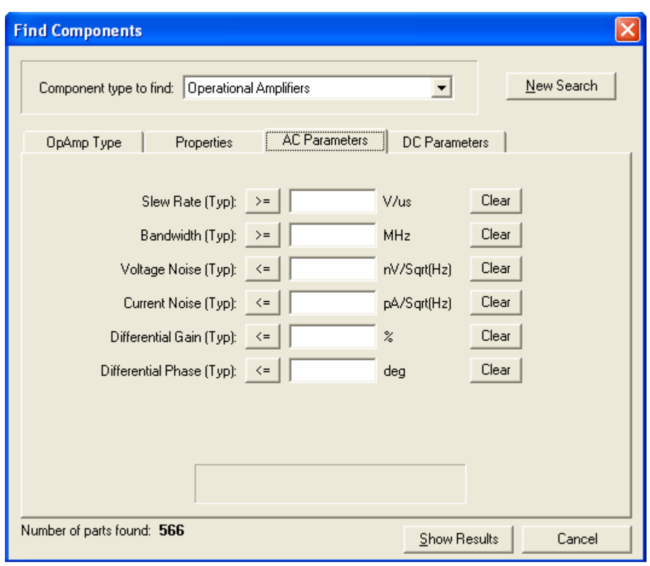

Figure 5.8 : A Snapshot from "Selguide" [17]

Selguide is a software tool designed to guide the user in selecting NSC operational amplifier, buffer and comparator products by enabling the user to enter in a few key parameters and have a list of devices meeting those parameters returned to them. The results are summarized in a table of key device parameters and pricing information, as well as a link back to view NSC web site product folders for the chosen devices.

We have made an extensive search from the op-amp manufacturers to find the ones with the best parameters interested such as the input-current noise, the input-voltage noise and the input capacitance. They are listed in the table 5.2 with their parameters.

Table 5.2 : Some Parameters of the Considered Op-amps

Op-amp	Input-Current Noise ($fA/\sqrt{Hz}$)	Input-Voltage Noise ($nV/\sqrt{Hz}$)	Input Capacitance (pF)
Burr-Brown (TI) OPA365	4	4,5	2
Burr-Brown (TI) OPA847	2500	0,85	1,7
Maxim-Dallas MAX4477	0,5	4,5	10
Linear Technology LTC6244	0,56	8	2,1

OPA847 in the list and LMH6626 (out of the list) were also considered because of their low input-voltage noise values and low capacitances. But none of them could detect gamma radiation because their input current noises are too high compared to the rest of them given in the table 5.2.

Gamma-rays from a Cs-137 source were observed very first time when using Hamamatsu S1223-01 photodiode and LTC6244 op-amp in the standard circuit of Maxim [18]. The 60 keV gamma-rays from Am-241 couldn't be observed because of the large noise level. The count rate from the Cs-137 was also relatively in the use of this op-amp. After this experience OPA365 op-amp were used and Cs-137 peak were observed nicely together with Am-241 peak. Although observed Am-241 line was too close to the noise level, it was observable by naked eye from the oscilloscope.

However the electronic discrimination between the noise and the Am-241 peak was quite hard.

Unfortunately all of the op-amps were produced in the SMD (surface mount device) format which makes the PCB design and soldering rather difficult.

For reducing the noise level, first the Faraday caging and then the cooling were experienced. Faraday caging dramatically improved the signal to noise ratio. Cooling the detector by locating the whole detector assembly into an ice box also improved the signal quality as expected. Here are the test conditions of these experiments.

OPA365 op-amp and Hamamatsu S1223-01 were used in this experiment under following conditions.

Supply voltage: $V_{cc} = + 5{,}02$ V,

Bias voltage: $V_{bias} = - 30{,}12$ V,

Current drained: $I_{cc} = 18$ mA.

Consequently, Am-241 peak at 60 keV was observed at 93 mV where the noise level of the detector circuit was 60 mV.

As a comment of this study, Faraday cage is strongly recommended for reducing the noise level since the electromagnetic wave sources from the other devices greatly contributes to the noise. Faraday caging will be discussed in the next chapter. Also reducing the operating temperature of the photodiode reduces the noise coming from thermal effects [19]

The same circuit was tried with the same photodiode and MAX4477 op-amp. The results were better than all other op-amps tried. The noise level of the circuit was 60 mV without faraday cage which means the even Am-241 peak could even be seen without a Faraday cage. Also the detection efficiency was relatively good for this case.

After all of these considerations and experiments, the most optimal op-amp for this detector circuit is found to be MAX4477 with its suitable input-current noise, voltage noise and capacitance value. Also the response time of the op-amp meets requirements for faster detection.

5.5 Digital Output

Sometimes, it is also necessary to determine the count rate of the radioactive source above a certain energy threshold. In this case a digital output from the detector (this output maybe connected to the clock signal of a counter) would be ideal. When a gamma photon is left deposition by the detector, an analog voltage peak appears in the output. Using a comparator, a one bit ADC, analog signal can be converted to a logic signal. In the original design, we observed a problem. Noise on the signal was also triggering the comparator causing more then one digital signal output generated instead of a single one for every gamma above the threshold. This problem was solved by using the negative input of the comparator. The negative part of the signal is smoother and effect of the noise is less visible there.

In electronics, a comparator is a device that compares two voltages or currents and switches its output to indicate which is larger. More generally, the term is also used for referring to a device that compares two items of data.

In the detector circuit, analog output of the amplifier stage is connected to the negative input of the comparator. The positive input is connected to the +5 V voltage supply by an adjustable resistor. So the comparator will compare these two signals and distinguish between the signal and noise. The basic operation logic and the schematics of the comparator are shown in Figure 5.9.

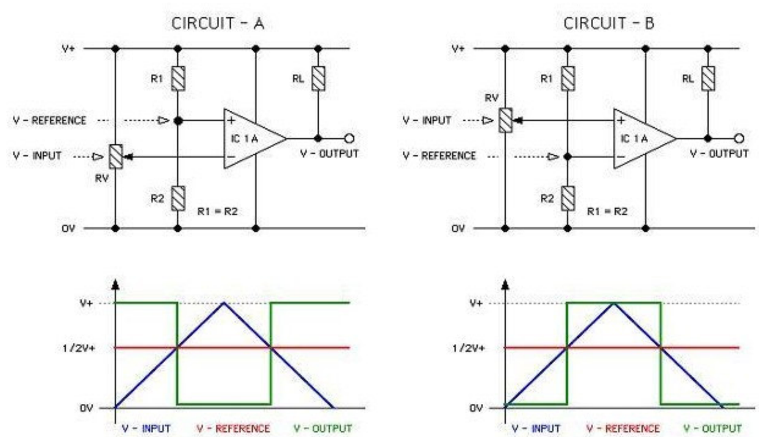

Figure 5.9 : Basic Operation of Voltage Comparators[20]

The amplifier's output will give an AC signal on the DC bias. This output is applied to the negative input of the comparator. The positive reference input signal can be arranged by an adjustable resistor. The arranged DC level is known as the threshold.

By arranging the resistor, positive reference signal can be set to little above the noise level of the circuit which means the noise will be rejected by the comparator and only the detected gamma signal above the noise will be converted to a digital logic pulse. Figure 5.10 shows analog and digital signals in the original circuit.

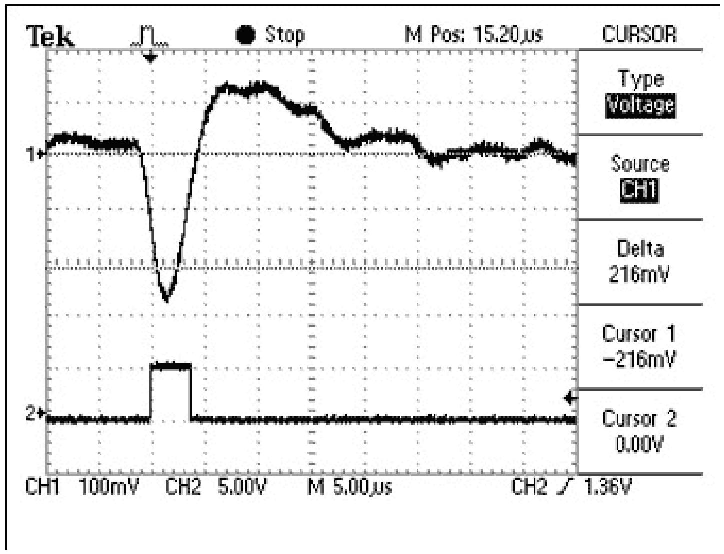

Figure 5.10 : Analog versus Digital Signal [18]

Because the comparator is at the end of the circuit, noise contribution to the signal is neglected. The most important selection criteria for the comparator will be the response time. Maxim's MAX987 comparator is suitable for this operation where some of the time characteristics are given below in table 5.3.

Table 5.3 : Some Characteristics of MAX987 Comparator[21]

PARAMETER	SYMBOL	CONDITIONS			MIN	TYP	MAX	UNITS
OUT Rise Time (MAX987/MAX991/ MAX995 only)	t_{RISE}	V_{CC} = 5.0V		C_L = 15pF		15		ns
				C_L = 50pF		20		
				C_L = 200pF		40		
OUT Fall Time	t_{FALL}	V_{CC} = 5.0V		C_L = 15pF		15		ns
				C_L = 50pF		20		
				C_L = 200pF		40		
Propagation Delay	t_{PD-}	C_L = 15pF, V_{CC} = 5V	MAX987/MAX991/ MAX995 only	10mV overdrive		210		ns
				100mV overdrive		120		
			MAX988/MAX992/ MAX996 only, $R_{PULL\text{-}UP}$ = 5.1kΩ	10mV overdrive		210		
				100mV overdrive		120		
	t_{PD+}	MAX987/MAX991/MAX995 only, C_L = 15pF, V_{CC} = 5V		10mV overdrive		210		
				100mV overdrive		120		
Power-Up Time	t_{PU}					25		µs

5.6 Final Amplification Stage

Another amplification stage can be added to the detector circuit for additional purposes. The main purpose of this final amplification stage is to connect our detector output to a multi channel analyzer (MCA). The final amplifier stage also should resolve the impedance disagreement between the MCA input and the output of the detector circuit. The final amplifier stage can be added to the analog output of the amplifier which is normally connected to the negative input of the comparator. After the amplification of the output signal, both the signal and the noise will be amplified. Thus S/N will not change as long as amplifier noise is not bad. The amplifier is made from an audio amplifier TDA2030 [22]. Either single or split power supply can be used for this amplifier. The schematics of the final amplifier stage can be shown in Figures 5.11a and 5.11b where a split and a single power supplies are used respectively.

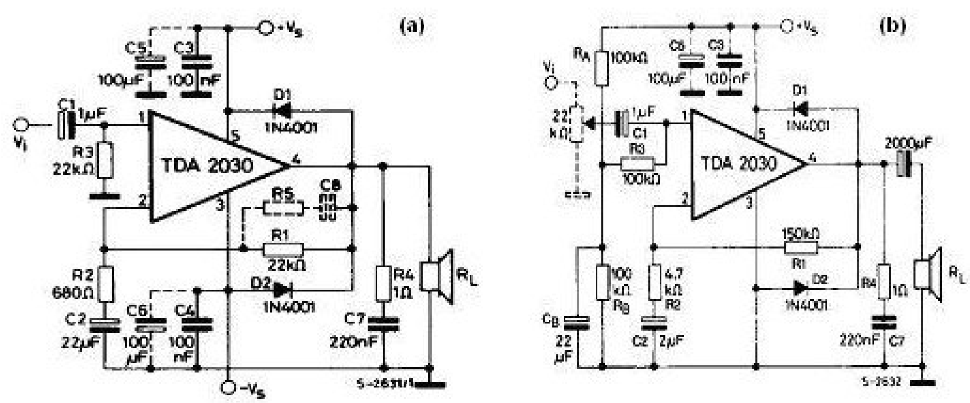

Figure 5.11 : **a)** Split Supplied Amplifier[22] **b)** Single Supplied Amplifier[22]

Figure 5.12 and 5.13 shows the comparison of unamplified and amplified signals from the radioactive sources of Cs-137 and Am-241. As can be shown from these figures, the signal trend doesn’t change with the amplification which proves the bandwidth of the TDA2030 is good enough.

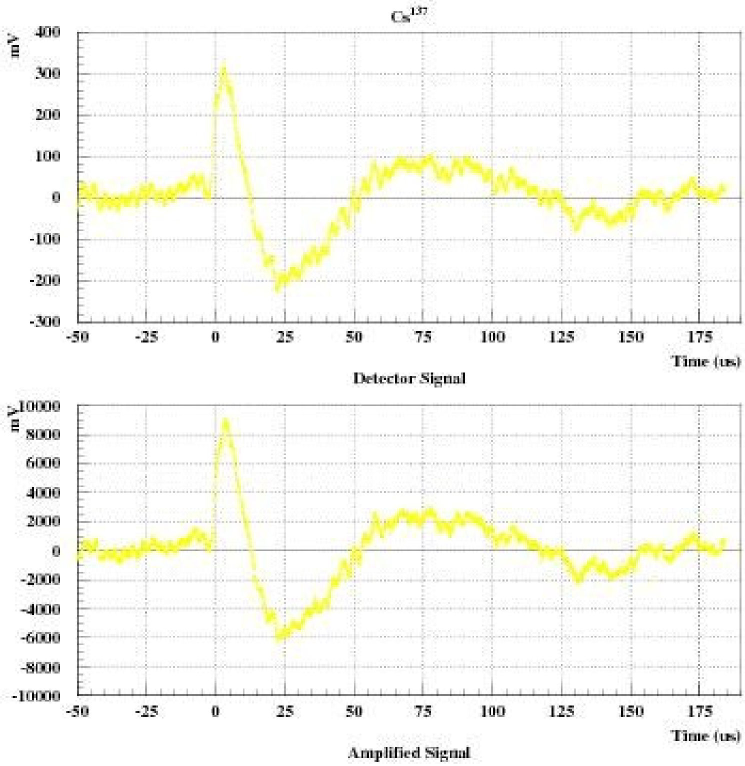

Figure 5.12 : Unamplified and Amplified Signals from Cs-137

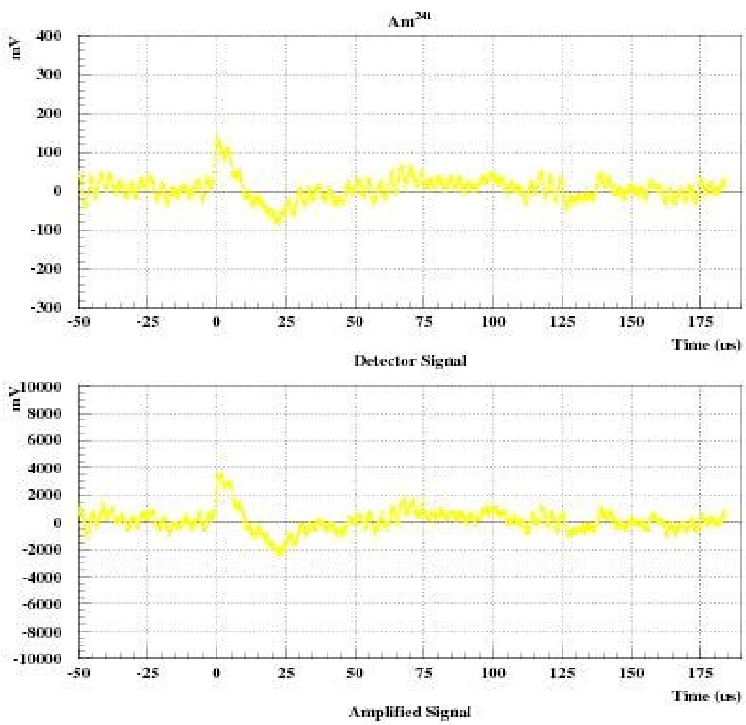

Figure 5.13 : Unamplified and Amplified Signals from Am-241

6. EXPERIMENTAL SECTION – DETECTOR CIRCUIT CONSTRUCTION

In this section, detector construction and the modifications made in the circuit will be explained. The sample detection circuit is taken from the application note of Maxim Dallas Company[18]. This circuit is more or less standard for this kind of applications. As we discussed in the previous chapter, the circuit contains a transimpedance amplifier, the shaping amplifier and the comparator sections. However optimization took place and some of the circuit elements were replaced with the more suitable ones. Figure 6.1 shows the main circuit diagram.

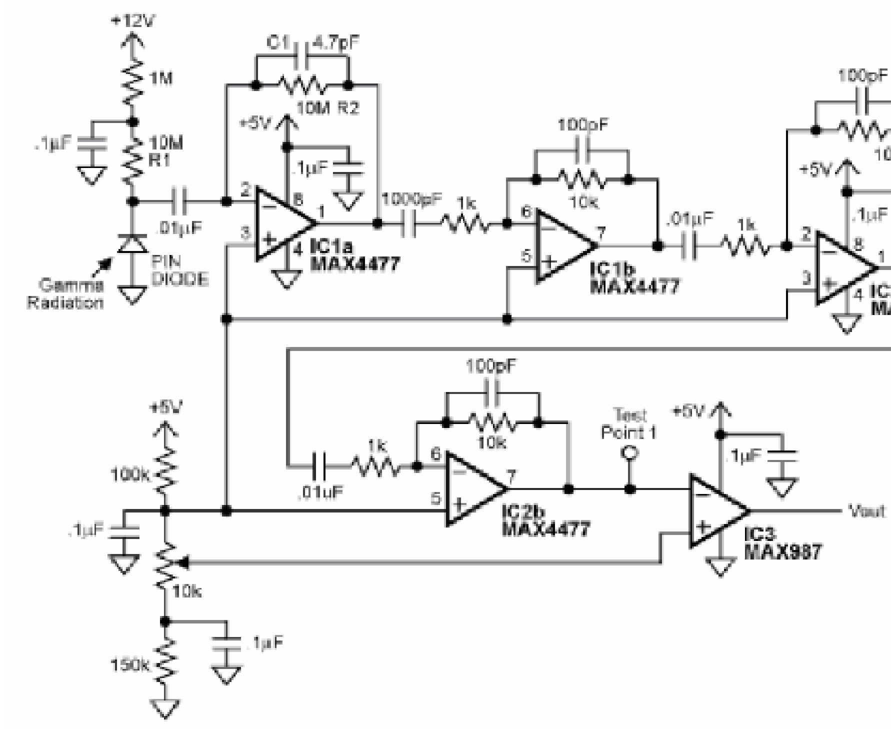

Figure 6.1 : Original Detector Circuit [18]

6.1 Construction of the Detector Circuit

Construction of the detector circuit is a quite a long time process with a lot of trial and error. We started with designing the printed circuit board (PCB). We used Eagle 4.16r1 layout editor [23]. The PCB design requires some considerations.

The very first one is to choose the signal paths as short as possible. Longer lines mean more parasitic capacitance and more noise. The parallel long lines close to each other can also cause “crosstalk” between the two lines. If two-sided PCB design is considered, the number of transitions between the layers have to be minimized. Our detector circuit contains 4 op-amps, a comparator, and 24 passive circuit elements with an adjustable potentiometer. Our very first design was based on limiting the width of the PCB to the width of the photodiode and making it long as it necessary. The purpose of this design was to have better packing factor so the individual detectors can be mounted close to each other. However this design was required to use a two layer design with very thin and close lines with many jumps (transitions between the two layers). There were a lot of problems in this design. Unfortunately only very few out of many constructed detectors ran properly. Designing the circuit with minimum jumps and with thicker lines made the construction easier and more trustable. Figure 6.2 shows one of the PCB design made with EAGLE, Cadsoft [23].

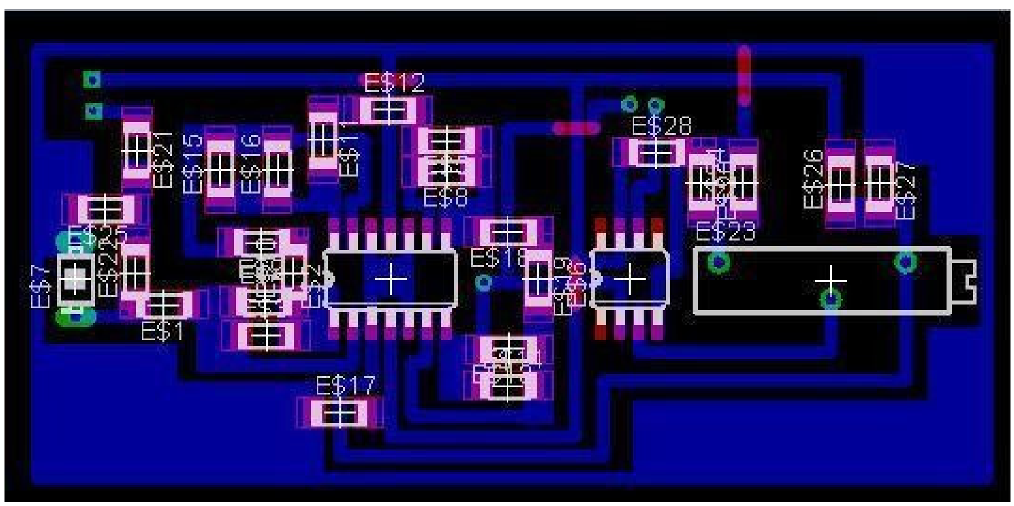

Figure 6.2 :   Detector Circuit Designed with Eagle 4.16r1

After the design was completed with Eagle, the layout was printed out on a special paper called PNP. The laser printed circuit paths (the blue connection lines shown in Figure 6.2) can be transferred on to the copper clad under the heat and the pressure applied by a standard iron. After the copper clad is cooled down, PNP is pealed off and clad is put into a hydro-chloric acid and the hydrogen peroxide mixture. The lines transferred on to the copper clad do not get in to any reaction with acid mixture. After all other sections (naked copper) dissolve in the acid, PCB is ready.

A temperature adjusted solder station with static discharge protection should be used for the soldering process. The soldering temperature should not exceed the limits given in their data sheets of the device components. A clean work is absolutely necessary. The size of the detector PCB is smaller in the final design (4.1 cm x 2.9 cm). Soldering the SMD (Surface Mount Device) circuit components is not trivial and requires experience. When the soldering process is completed, construction of the Faraday caging begins.

Figure 6.3 shows one of the constructed detector with the comparator's inputs inverted. Note that the passive elements in this one are not SMD's. We used SMD components in all of the 16 detectors.

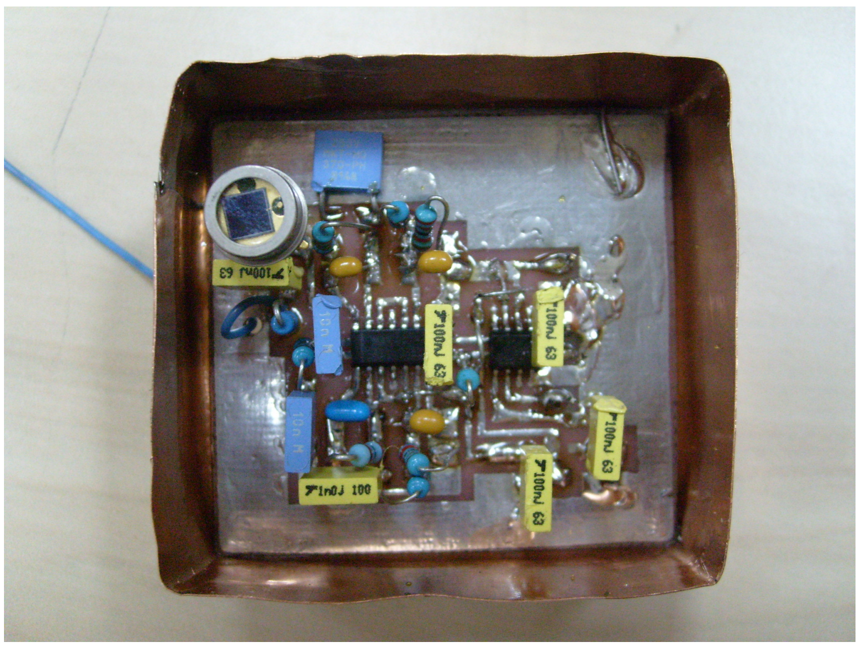

Figure 6.3 : Typical detector constructed

Detectors drain approximately 10 mA current from the power supply. Most of the time, any misoperation can be identified by any deviation from 10 mA current. After constructing 16 detectors, all these detectors are put close together to form a gamma ray detector array as shown in Figure 6.4 and 6.5.

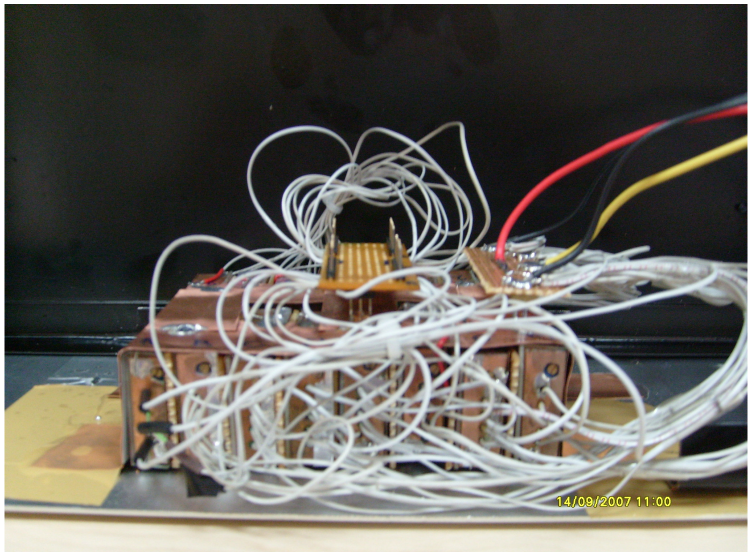

Figure 6.4 : Gamma-Ray Detector Array (back)

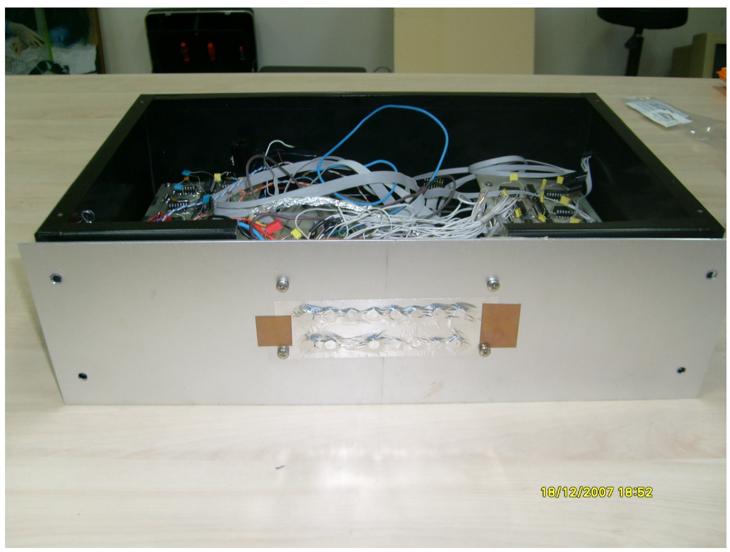

Figure 6.5 : Gamma-Ray Detector Array (front)

Another important point at the construction is to provide a stable bias voltage. If the bias supply is noisy, the noise sneaks into the photo-diode and detected as photo current. The best noise free bias supply is a battery. But finding a battery with 30 V is not trivial. For that reason we decided to use a laboratory grade regulated power supplies for both the power and the bias.

6.2 Digital Readout Design and Construction

Since we are interested in counting the gamma-rays from the detector array of 16, we need a digital interface circuit to transfer this data into a computer.

To transfer 16 bit of data into a computer is not trivial. If this data was only 8-bit, the parallel printer port would be ideal. For 16-bit, we used 8255 programmable peripheral interface [24]. This device can be programmed to have 24 bit input/output. Here is the procedure to transfer 16 bit data into a computer.

We used 16 8-bit counters (74LS393) to store the events from the individual detectors. A certain time is required to transfer the data from the detectors to the computer. In order to not to loose any events during this transfer process, the output of the individual detectors should be stored independently. When one of the detectors is read out by the computer, the content of the related counter is erased immediately and this process continues with the next counter. A buffer stage (74LS541) is also used for transferring the data from counters to the next stage of OR gates. Figure 6.6 shows this process for 4 counters. The PCB design of the digital readout system is shown in Figure 6.7. For 16 counters, 4 identical devices can be used and the outputs of these four is again combined properly using another OR gate logic. Figure 6.8 shows the block diagram of this device.

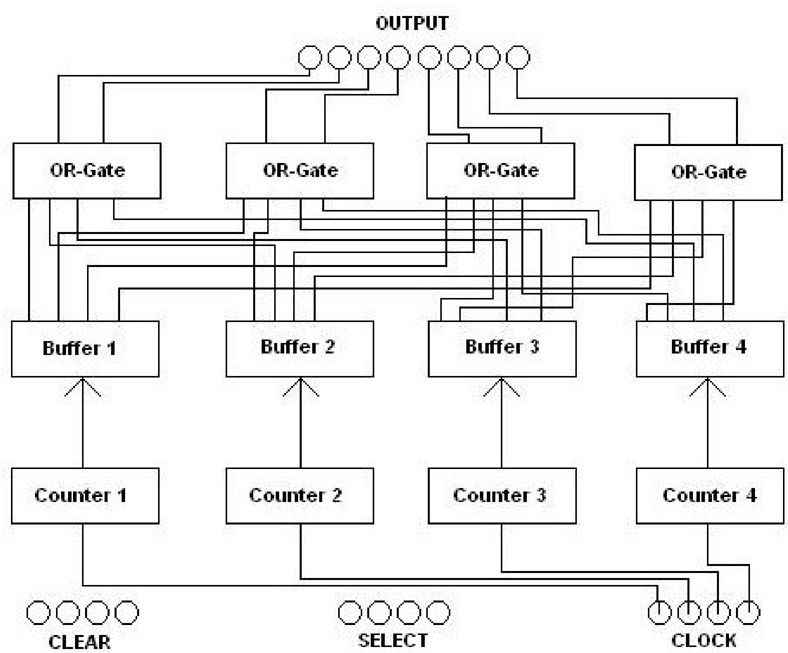

Figure 6.6 : Part of the Digital Readout System

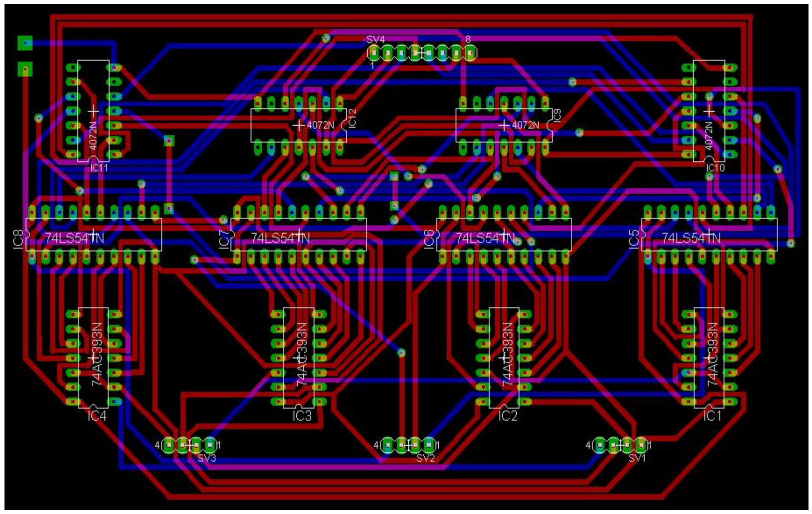

Figure 6.7 : Counter Part Design Made with Eagle 4.16r1. The Red and Blue Lines are Representing the Top and Bottom Layers Respectively

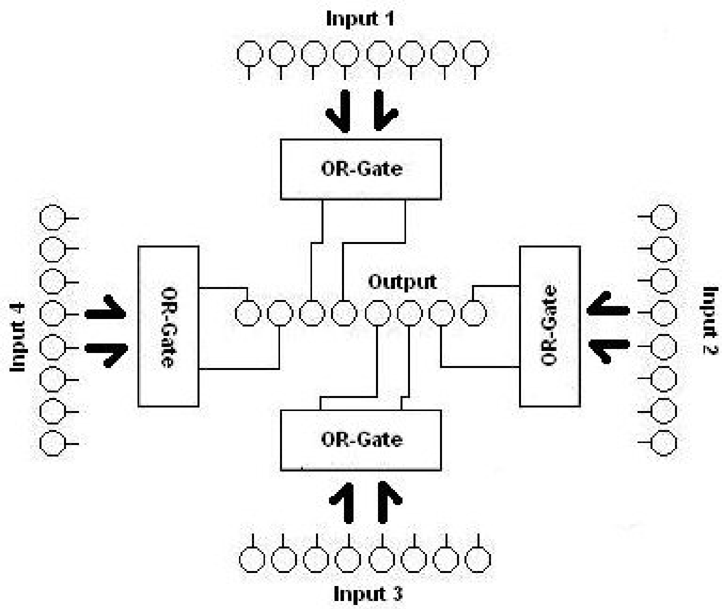

Figure 6.8 : OR-gates Combination of the Digital Readout System

6.3 Optimization of the Transimpedance Amplifier Stage

In the transimpedance section, the effect of the feedback resistor and the capacitance on the noise and the detection efficiency were experimentally studied. This study helped us to choose the best values of the feedback resistor and the capacitance.

In the following experiment, the value of C_1 was changed and the noise level and the detection efficiency of the circuit were measured. During this experiment, the top cover of the Faraday cage was open.

Table 6.1: Relation Between the Value of the Feedback Capacitance and the Noise. V_{cc} = 5,02 V, V_{bias} = -30,16 V , R_1 = 10MΩ , R_2 = 1,2MΩ

Feedback Capacitor C_1 (pF)	Noise Level (mV)
0,5	Goes into oscillation
1	50
1.5	70
4.7	78

It is known theoretically that the reducing the value of the feedback capacitance also reduces the noise level. From this experiment as shown in table 6.1, we decided to use C_1=1 pF. When replaced by 0.5 pF (the minimum value one can find in the market) the output goes to an oscillation.

We also changed the value of the R_2 resistor which is also on the signal path and observe how the detector efficiency and noise changes. For the observation of the efficiency, measuring the count rate is proper. The count rate is observed directly from the frequency counter of the oscilloscope. Since this measurement is strongly depend on the Volt/Div value of the scope, this parameter is given in the table 6.2.

Table 6.2: The Relation Between the Value of the Bias Resistor and the Noise Efficiency. Test Conditions are: V_{cc} = 5.02 V, V_{bias} = -30.2 V, R_1= 10 MΩ and C_1= 4,7 pF, Volt/Div = 0.2 V, t_b=t_g= 60 s and Source is Cs-137

Bias Resistor (R_2) (MΩ)	Background	Gross
1.2	415000	510000
3.9	504000	515000

As the result of this experiment, we observed that change in the R_2 resistor doesn't affect the gross count, but it affects the background counts. Optimum value of the feedback capacitance and bias resistor are found to be 1 pF and 1.2 MΩ respectively.

6.4 Optimization of Shaping Amplifier Stage

The shaping amplifier of the detector contains three amplifier stages connected in series. The 10 kΩ input resistors are left their initial value. The feedback capacitors at the shaping stages were tuned to get the highest efficiency. By looking at the noise level and the detection efficiency, the optimum value of the C_1, C_2 and C_3 capacitors were determined. The first experiment took place with the initial value of the feedback capacitance (4.7 pF) in the transimpedance stage. The data of this study is given in table 6.3.

As a result of this experiment, it can be seen from the table 6.3 that the values C_1=200 pF, C_2=147 pF and C_3=147 pF gave the maximum count rate.

Table 6.3: Optimization of the Shaping Amplifier. C_0 = 4.7 pF, V_{bias}= -30 V, V_{cc}=5 V, Counting Time = 1 Minute. All Capacitors are Given in pF

C_1	C_2	C_3	Counts from sources				Background
			Cs-137	Am-241	Co-60	Ba-137	
100	100	100	6430 6422	407 399	812 797	1169 1131	11
147	100	100	6712 6842	354 366	859 895	1154 1137	8
147	147	100	7190 7226	597 634	891 954	1354 1375	19
147	147	147	7890 7857	821 799	975 994	1298 1338	12
200	147	147	7867 7787	1001 986	1077 1048	1268 1275	14
200	100	100	6640 6662	640 647	946 901	1235 1201	14

Similar experiment was repeated by changing the feedback capacitor C_0 from 4.7 pF to 1 pF.

Recalling the optimization of the transimpedance amplifier, C_0=1 pF gives the best result.

Table 6.4: Re-optimization of the Shaping Amplifier. C_0 = 1 pF V_{bias} = -30 V, V_{cc}= 5 V and Counting Time = 1 min. All Capacitor Values are in pF

C_0	C_1	C_2	C_3	Counts from sources Cs-137	Am-241	Co-60	Ba-133	Background
4.7	200	147	147	8400	1500	1300	1760	118
1	200	147	147	8500	1620	1220	1900	36

Change in the count rate of Am-241 and Ba-133 is close to 5σ when backgrounds are taken into account [25]. This is a significant change. Cs-137 and Co-60 don't show any significant change. The reason for that is both Am-241 and Ba-133 have intense low energy X and gamma-rays close to the noise threshold of our detector. Therefore any work in favor of improving S/N ratio will reflect to the count rate for these sources.

6.5 Photodiode Tests

Some tests were performed on the photodiode to increase the overall efficiency of the detector. Here are these tests:

It was told previously that the thickness of the depletion region of the photodiode rises with the increasing applied bias voltage. We studied the effect of the bias voltage on the detection efficiency. In this study, bias voltage was changed and corresponding count rate is measured.

Resistor R_1 is a large resistor for limiting the dark current. As we know, the noise in a resistor is proportional with the square root of its value. Therefore larger resistor can introduce more noise. In this test, both for 10 MΩ and 20 MΩ of the value of R_1, the bias voltage was changed and corresponding count rate was measured. For the measurement of the count rate, oscilloscope settings were Volt/Div=0.5 V and time setting was 0.1 ms. A Cs-137 source was used in this study. The data collected for this purpose is shown in Table 6.5.

As a result of this test, it was proved that the smaller the R_1 is the larger the count rate is. The noise increases with the resistance. However, increasing noise forces the threshold to be increased too. Thus, smaller peaks as a result of small energy deposition are lost. Table 6.5 proves this.

Table 6.5: Bias Voltage versus Count Rate Taken with Cs-137

Bias Voltage (V)	Counts/min	
	R_1 = 20 MΩ	R_2 = 10 MΩ
-30	1051	1250
-25	987	1040
-20	945	1100
-15	921	960
-12.5	925	850
-10	822	890
-7.5	798	790
-5.0	693	740
0	335	440

Figure 6.9 shows the applied bias voltage vs count rate of Cs-137 for both R1 and R2

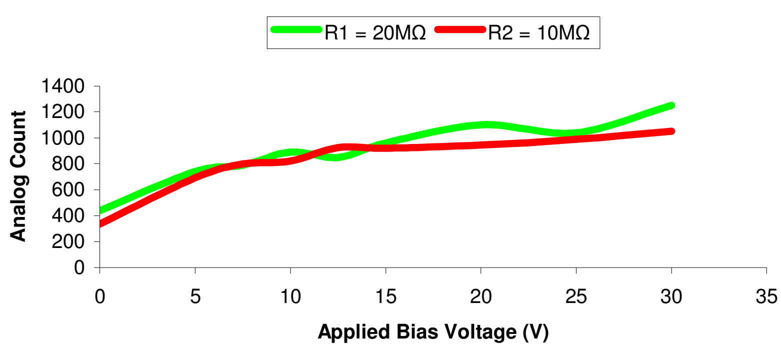

Figure 6.9: Applied Bias Voltage versus Count Rate for Different Resistors

6.6 Faraday Caging

Faraday caging is one of the most important part of the construction for reducing the noise level. An external electrical field will cause the electrical charges within the conducting material to move or redistribute them. Faraday cages also shield the interior from the external electromagnetic radiation if the conductor is thick enough and any holes are significantly smaller than the wavelength of the electromagnetic interference.

The very first detector circuit we had constructed was not in Faraday cage. Noise level of it was measured at 93 mV. Since the noise level was too high, 60 keV line of Am-241 was not able to be observed. All of our 16 detectors were shielded with Faraday cage.

A single layer PCB design was preferred for the reasons mentioned before. However for the production of the PCB's we used two layers. The unused bottom layer of the PCB was used as one of the side of the Faraday box. For the other sides of the Faraday box, double sided copper clads were cut properly and connected in the shape of a matchbox. All surfaces (inner and outer) are soldered to each other and to the ground. Figure 6.10 shows one of the detectors with Faraday cage used for the test purposes. Here we used a copper tape located side by side and soldered in between as seen from the figure. The noise level was reduced to the 50 mV level which was enough for observation of the 60 keV gamma line of Am-241. Black mark shows the location of the photodiode.

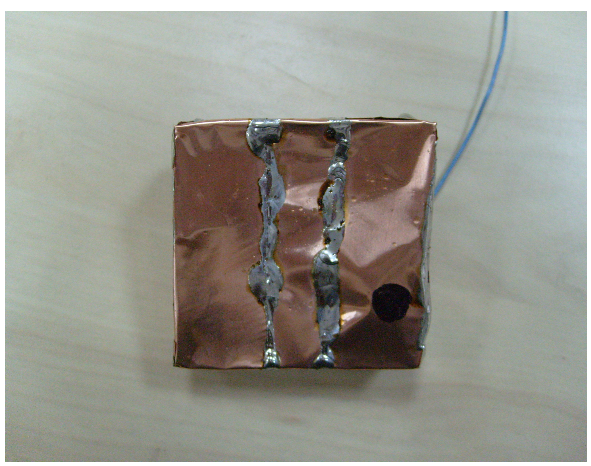

Figure 6.10 : Detector with Faraday Cage

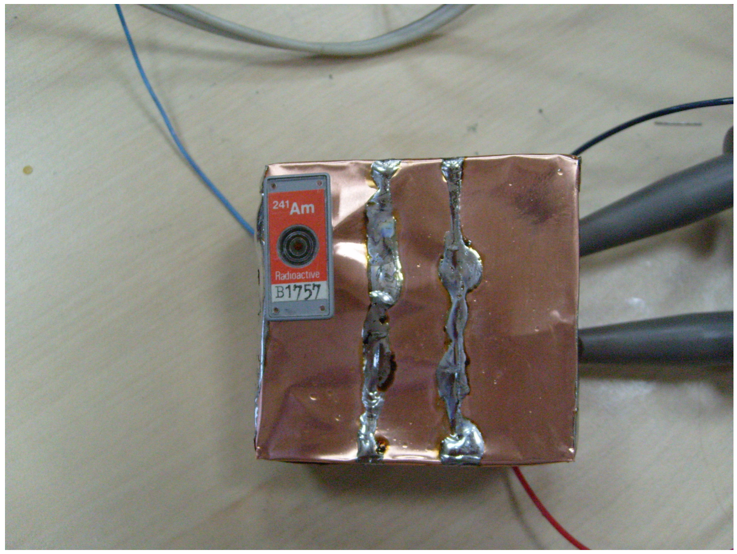

Figure 6.11 : Am-241 Source is Located on the Photodiode and Detector is Ready

Figure 6.12 : Detected Am-241 Peak with Digital Output

As seen in Figure 6.12, Am-241 peak is too close to the noise level. Therefore Faraday caging is a "must" for observing the signals from small energy depositions. The digital signal is trigged by the falling edge of the analog signal.

6.7 Comparison of Gamma-Rays from Various Sources

Here are some of the observed signals from various radioactive sources. Figure 6.13 shows the signal from Cs-137.

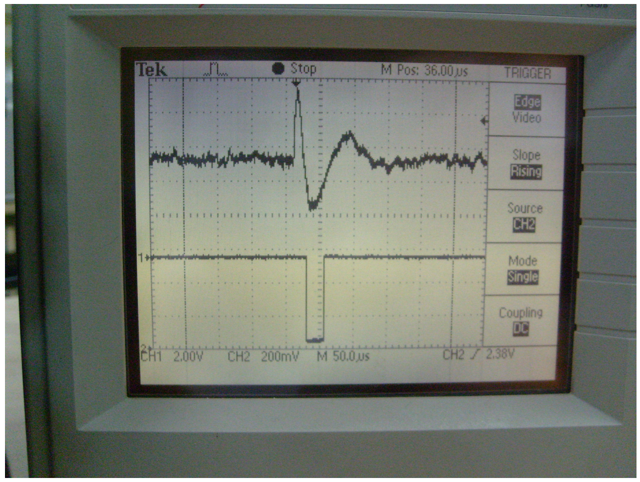

Figure 6.13 : Detected Gamma-Ray Signal from Cs-137

Unfortunately the resolution time of the detector is not so great. Full waveform from a single event takes almost 100 μs time. However sometimes one scope trigger can catch two events on the same screen (Figure 6.14.).

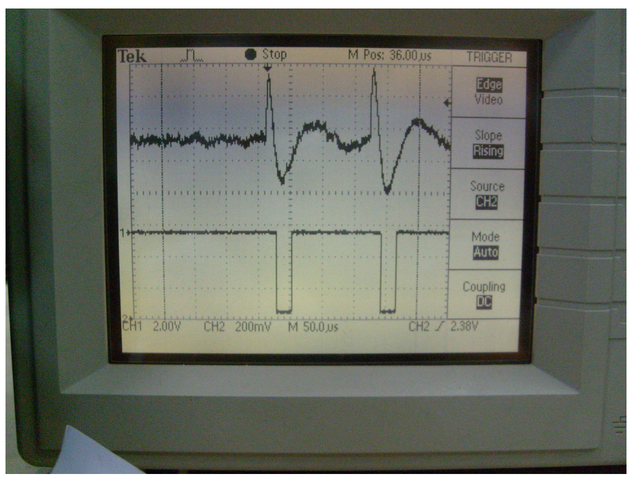

Figure 6.14 : Two Sequential Gamma-Rays Arrive within 150 μs

A GPIB interface from Tektronix TDS220 and WaveStar software [26] were used for dumping the signal waveforms into a PC. This enabled us to analyze the detector data better. Average of 10 detection signals from different radioactive sources were taken and combined in the same graph. Figure 6.15 shows this procedure. Here one can see there is nice correlation between the peak energies and the signal heights.

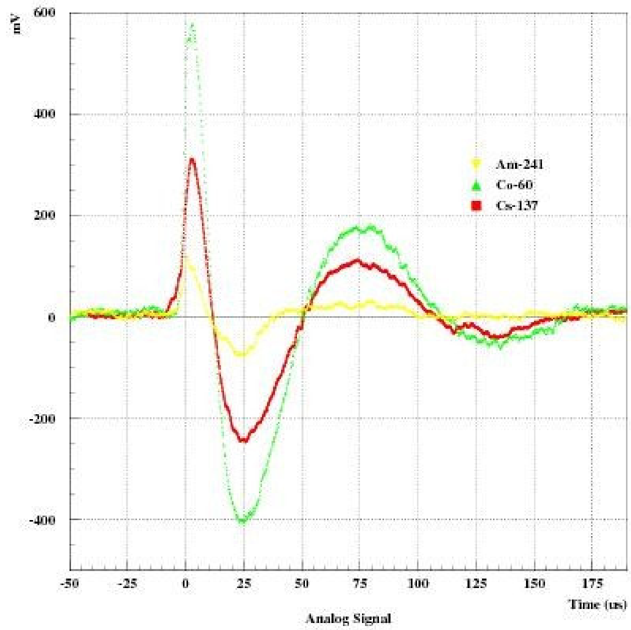

Figure 6.15 : Average of Ten Signals for Various Radioactive Sources

Figure 6.16 shows the energy of the incident gamma-rays versus total absolute area of the output signals. As seen from the graph, the relation is not linear. We know linearity is not good in the photoconductive type of connection. There is a useful information can be extracted from this study. Comparison between the straight line and the fit shows the relative efficiency between the 661 keV and 60 keV is around 0,5. In other words, the efficiency at 60 keV is two times larger than the one at 661 keV.

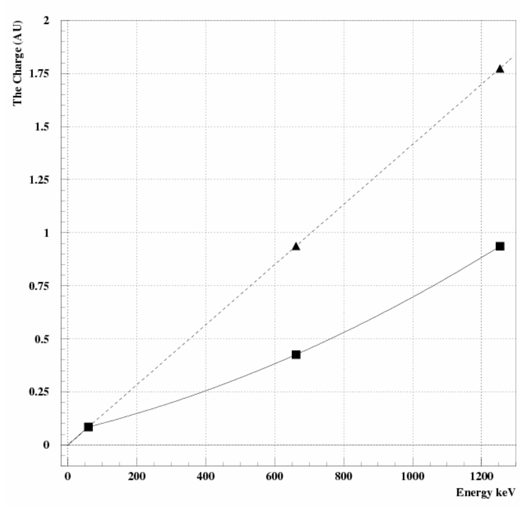

Figure 6.16 : Relative Comparison of Efficiencies Between Various Energies

6.8 Noise Analysis of the Detector Circuit

Noise signal of the detector can be defined as the output when there is no radioactive source near the detector. Figure 6.17 shows a typical noise signal sampled from the oscilloscope when there is no radioactive source nearby. The Tektronix TDS220 oscilloscope is 100 MHz and capable of handling 1 GS/s. In the Figure 6.17, the data was taken with 2500 points with 4 μs resolution. This enables us to analyze the noise data between 0 to 125 kHz. This bandwidth is actually much smaller than 10 MHz bandwidth of the op-amp. However it is good enough to see if there is any low frequency noise component in the detector output.

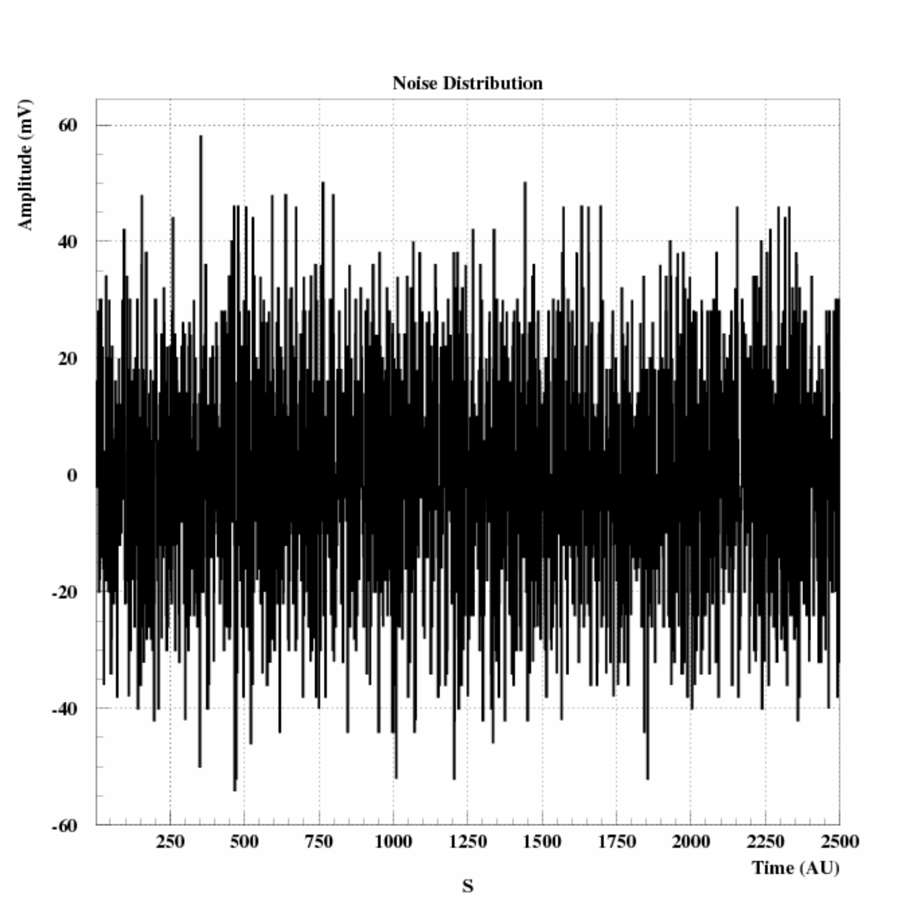

Figure 6.17 : Snapshot of the Noise Taken from Detector

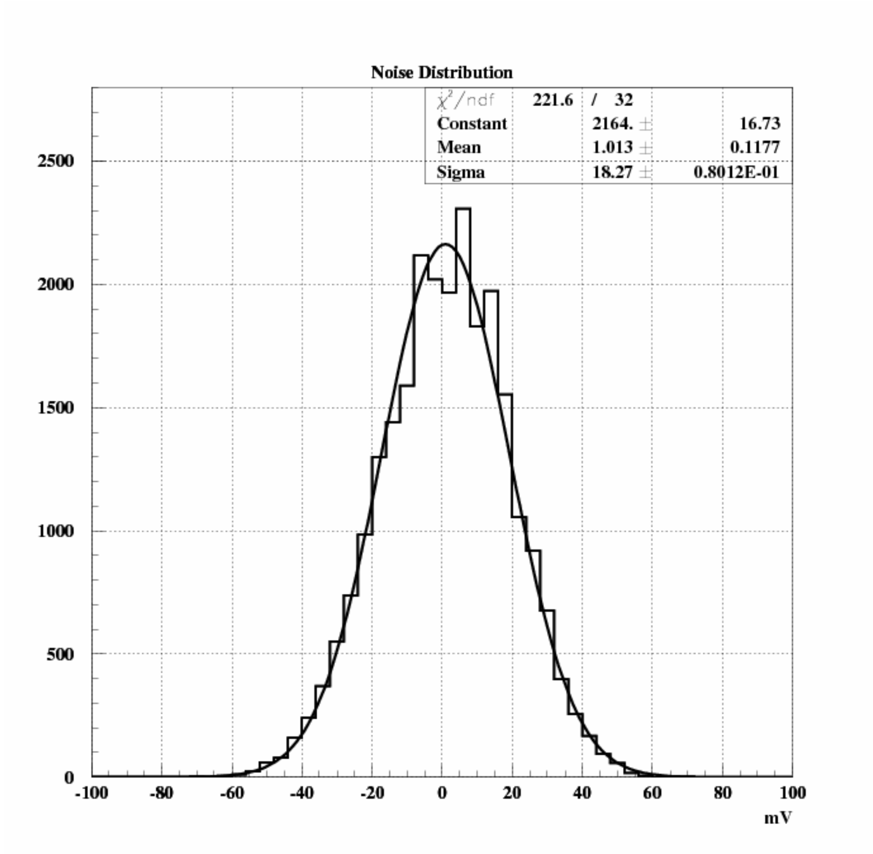

Figure 6.18 : Noise Distribution

As can be shown in Figure 6.18, the noise distribution of the detector circuit is in good agreement with the Gaussian distribution which means that dominant noise factor comes from the thermal and shot noise. As explained in the theoretical section, thermal and shot noise shows random structure.

The root mean square (RMS) value of the noise distribution is found to be 18 mV which means that the average noise of the detector circuit is 55 mV when 3σ is considered.

Figure 6.19 shows the Fourier spectrum of the noise. As can be shown in figure, there are some peaks at 9.92 kHz, 50.1 kHz, 60.02 kHz, 69.94 kHz, 110.02 kHz and 120.04 kHz. It looks like the 9.92 kHz and 60.02 kHz peaks seem to be real. 50.10 kHz and 69.94 kHz peaks may be due to the beatings between these two main peaks. 110.02 keV may be generated from the beating between 50.10 kHz and 60.02 kHz and similarly 120.04 kHz is from the beatings between 50.10 kHz and 69.94 kHz. Honestly we have no idea about where these noises come from. It should be investigated.

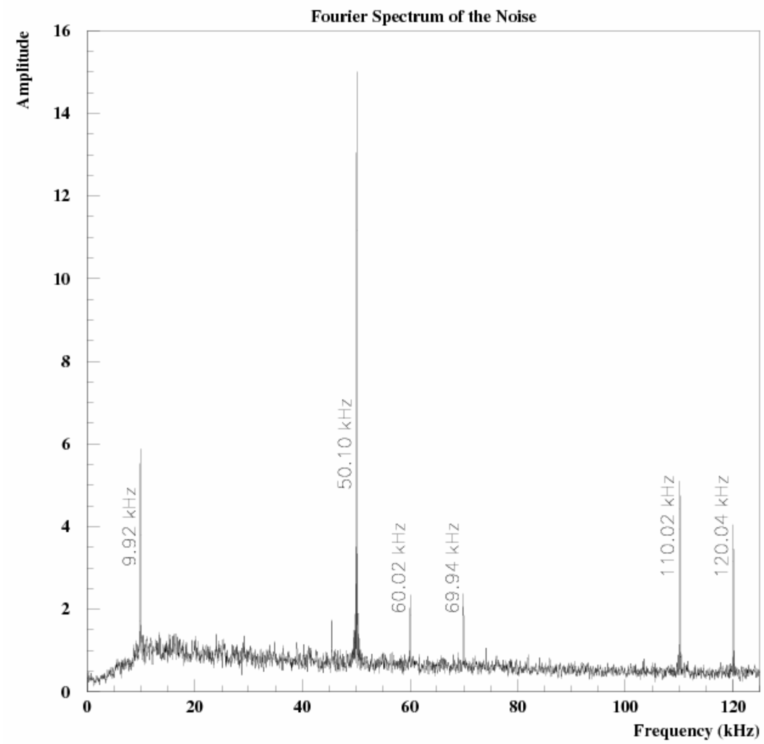

Figure 6.19: Fourier Spectrum of the Noise

6.9 Interfacing the Detector Array Data to the Computer with 8255

8255 programmable peripheral interface is a chip manufactured by INTEL Company for establishing the communication of the peripherals with central processor unit (CPU). This chip can be used for 24 bit input/output of the binary information. We will not give the details about this card. However these cards were constructed in the department for the laboratory usage of microprocessors course.

8255 has three ports; Port A, Port B and Port C. Each has capable of making 8 bit data I/O. We mentioned before that we built necessary logic device for porting 16 digital data from detector array to the computer. In this logic unit there are 16 clear signals controlling the counters, 16 select signals controlling the buffers and 8-bit counter information from individual counters. Total number of bits to deal with is 40.

Since a single 8255 interface card has a capacity of handling 24 bits, it’s needed to use two 8255 interface cards. Figure 6.21 shows the distribution of 40 bits between the two interface cards. The information of “clear” and “select” are provided by the computer.

This means B and C ports should be programmed as output and these outputs are connected to the related section in the logic control board. Similarly data is read from the Port A of the interface card 1 and for that reason Port A of the interface card 1 is programmed to be an input. This procedure is shown in the Figure 6.21 schematically.

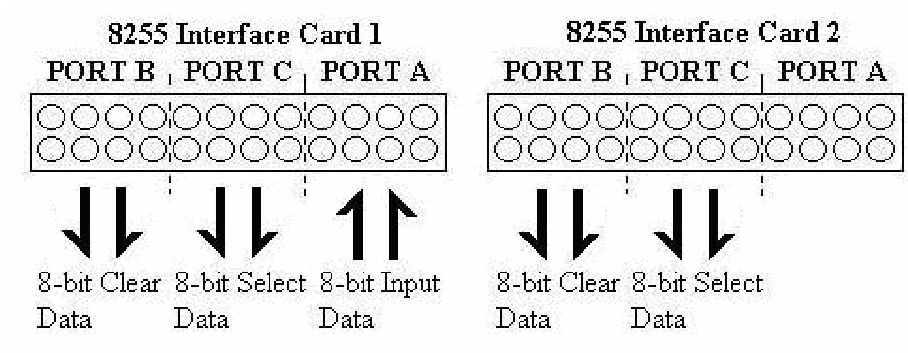

Figure 6.20 : Distribution of 40 Bits in Two 8255 Interface Cards

6.10 Control Software

We used standard C programming language on Linux operating system [27]. Accessing the ports in Linux is only possible in super user mode because of the security reasons. Therefore this code should be compiled and run as "root".

Flow chart of the program is quite simple and can be summarized as follows: All of the counters are reset in the very beginning. Then, the software activates the first buffer. This transfers the 8-bit counter content of the first detector to the Port C of the first 8255 interface card. This 8-bit data is then read. Next, the software sends a clear signal to the first counter and goes in to the next counter. This process goes on until the counter 16 is completed. After that the operation restarts from the counter one. It should be noted that, when the computer is dealing with one of the counter, all other counters are independently counting the incoming radiation.

7. RESULTS AND DISCUSSION

As we mentioned in the introduction, the purpose of this study was to build a low cost gamma-ray detector produced from on-shelf components. We not only successfully produced this detector but also optimized it and determined the conditions for higher efficiency. We produced 16 of them, successfully tested and constructed a detector array from them. We designed a readout system for interfacing the array elements to a computer and tested the communications of each interface modules with the computer. This system actually is the base of an imaging detector used in nuclear medicine. The difference is, they have better resolution and efficiency. We believe this is probably the first time in Turkey such a project is completed from the stratch. The efficiency of the detector is small. However, for the cases where not much efficiency is needed, for instance for the monitoring of the bulk activity, this detector is ideal. Because it is really cheap, hundreds of them can be produced and located to the areas of interest. Since the power consumption is very small and the size of it is in the size of a matchbox, it can be used for battery operated personal monitoring device. The best of all is, this is a starting point for us to design and improve our own X and gamma-ray imaging detector in the future. Of course there is a lot of work to be done. Reducing the dead time and increasing the detection efficiency further more is important. Cooling the detector system to able to detect X-rays down to couple of eV will also be ideal in the future. Implementing digital counters to the detectors will be also very useful. That way the detectors can be located in the basements of the houses, in the mines or in anywhere the monitoring of natural the radioactivity is worth of. The window of the PIN diode can be removed to detect the charged particles. This might be useful for the experiments in high energy physics. We would like to have a TUBITAK support to improve this detector and to be able to materialize our future plans.

REFERENCES

[1] **Knoll G.F.**, 2000. Radiation Detection and Measurement 3rd Edition, John Wiley&Sons Inc., U.S.A

[2] **Hamamatsu**, Photodiode Technical Information

[3] **PerkinElmer Optoelectronics**, Application Notes

[4] **Nicholson P. W.**, 1974. Nuclear Electronics, John Wiley&Sons, Great Britain

[5] **Osi Optoeletronics**, 2003. Photodiode Technology

[6] **Kim, E.,** Primer on Photodiode Technology, University of San Diego, U.S.A

[7] **Rako, P.**, 2004. Photodiode Amplifiers – Changing light to electricity, National Semiconductors

[8] **Jung, W.**, 2005. Operational Amplifier Applications Handbook, Elsevier Print, U.S.A

[9] **Manchini, R**., 2002. Op-amp's for everyone – Design Reference, Texas Instruments

[10] **Spieler, H.**, 2002. Measurements-III Electronic Noise, ICFA Instrumentation School, İstanbul

[11] **Burr-Brown**, 1994. Integrated Circuit Applications Handbook, U.S.A

[12] **Philips Photonics,** 1994. Photomultiplier Tubes – Principles & Applications, Brive, France

[13] **Kittel C.,** 2005. Introduction to Solid State Physics, John Wiley&Sons , U.S.A

[14] **Hamamatsu Photonics K.K**., June 1993. Silicon Photodiodes and Charge Sensitive Amplifiers for Scintillation Counting and High Energy Physics, *Solid State Division, Catalog #KOTH0002E02*

[15] **Moses W. W., Derenzo S. E.,** 1994. Design studies for a PET detector module using a PIN photodiode to measure depth of interaction, *IEEE Transactions on Nuclear Science NS-41, pp. 1441–1445, LBL–34873*

[16] **Hamamatsu S-1223 Datasheet,** http://www.alldatasheet.co.kr/datasheet-pdf/pdf_kor/131548/HAMAMATSU/S1223.html

[17] **National Semiconductors,** Selector Guide Program *http://www.national.com/appinfo/amps/amplifiers_selection_guide.html*

[18] **Maxim/Dallas Semiconductor**, 2003. Application Note 2236, Gamma-Photon Radiation Detector

[19] **Inoue Y., Moriyama S., Hara H., Minowa M., Shimokoshi S.**, 1995. A liquid-helium cooled large-area silicon PIN photodiode x-ray detector, *arXiv:hep-ex/9504010v1*

[20] **Model Railroad & Misc. Electronics,** Voltage Comparator Information and Circuits, http://home.cogeco.ca/~rpaisley4/Comparators.html

[21] **MAX987 Datasheet,** http://www.ortodoxism.ro/datasheets/maxim/MAX987-MAX996.pdf

[22] **TDA2030 Datasheet** *http:/www.ortodoxism.ro/datasheets/stmicroelectronics/1458.pdf*

[23] **CadSoft**, Eagle Layout Editor 4.16r *http:/www.cadsoft.de/cgi-bin/download.pl?page=/home/cadsoft/html_public/download.htm.en&dir=eagle/program/4.1*

[24] **82C55A Datasheet**, *http://www.datasheetarchive.com/pdf/496740.pdf*

[25] **Bevington P. R., Robinson D.K.**, 2003. Data Reduction and Error Analysis for the Physical Sciences, U.S.A

[26] **Tektronix**, WaveStar Software for TDS220 *http:/www2.tek.com/cmswpt/swdownload.lotr?ct=SW&cs=sup&ci=5179&lc=EN&wt=480&wtwi=5179&wtla=EN&wtty=SW&wtsty=Update&wtpt=DOWNLOAD&wtsize=21+MB&wtver=1.0&wtcat=tektronix&wtti=WAVESTAR+UPGRADE+FOR+TDS+OSCILLOSCOPES*

[27] **Negus C.**, 2003. Red Hat Linux Bible, Wiley Publishing, U.S.A

PERSONAL BACKGROUND

Ekrem Oğuzhan Angüner was born in 1982, İstanbul. Graduated from Özel Batı Lisesi in 2000. After graduation from Hacettepe University at 2004 as a Physics Engineer, he started master degree in İstanbul Technical University in 2005.